The Colors of Dwarf Elliptical Galaxy Globular Cluster Systems, Nuclei and Stellar Halos

Jennifer M. Lotz [1], Bryan W. Miller [2], and Henry C. Ferguson [3]

ABSTRACT

We present the results of a Hubble Space Telescope WFPC2 F555W and F814W survey of 69 dwarf elliptical galaxies (dEs) in the Virgo and Fornax Clusters and Leo Group. The $V - I$ colors of the dE globular clusters, nuclei, and underlying field star populations are used to trace the dE star-formation histories. We find that the dE globular cluster candidates are as blue as the metal-poor globular clusters of the Milky Way. The observed correlation of the dE globular cluster systems' $V - I$ color with the luminosity of the host dE is strong evidence that the globular clusters were formed within the the halos of dEs and do not have a pre-galactic origin. Assuming the majority of dE clusters are old, the mean globular cluster color- host galaxy luminosity correlation implies a cluster metallicity $-$ galaxy luminosity relation of $\langle Z_{GC} \rangle \propto L_B^{0.22 \pm 0.05}$, which is significantly shallower than the field star metallicity - host galaxy luminosity relationship observed in Local Group dwarfs ($\langle Z_{FS} \rangle \propto L^{0.4}$). The dE stellar envelopes are $0.1 - 0.2$ magnitudes redder in $V - I$ than their globular clusters and nuclei. This color offset implies separate star-formation episodes within the dEs for the clusters and field stars, while the very blue colors of two dE nuclei trace a third star-formation event in those dEs less than a Gyr ago.

Subject headings: galaxies: dwarfs —galaxies: nuclei — galaxies: star clusters — galaxies: stellar content — galaxies: evolution — clusters: individual(Virgo, Fornax, Leo)

---

[1]Department of Astronomy and Astrophysics, University of California, Santa Cruz, CA 95064; jlotz@scipp.ucsc.edu

[2]Gemini Observatory, Casilla 603, La Serena, Chile; bmiller@gemini.edu

[3]Space Telescope Science Institute, Baltimore, MD 21218; ferguson@stsci.edu

1.   INTRODUCTION

It is generally believed that the dwarf galaxies we observe in the local universe are survivors of the hierarchical growth of massive galaxies. While present-day dwarf galaxies may somehow be different from the majority of proto-galactic fragments which coalesced into larger objects, the formation of stars in the smallest survivors are an important test of our understanding of galaxy formation and evolution. If star-formation quickly follows the gravitational collapse of the initial density perturbations in the early universe, we might expect the stars in dwarf galaxies to be quite old because their halos should be among the first objects to form. Dwarfs in large-scale over-densities destined to become clusters and groups should collapse and form stars at earlier times than galaxies formed in under-dense regions (Tully et al. 2002). Yet star-formation must not proceed too quickly, otherwise the baryons in the universe would become locked up in stellar remnants, leaving no fuel for the star-formation we see locally (e.g. Kauffmann, White, & Guiderdoni 1993).

Dwarf elliptical galaxies (and their low-mass Local Group analogues, dwarf spheroidals or dSphs) are an obvious place to look for ancient stars and to track early star-formation. dSphs and dEs in the Local Group are almost completely free of gas and typically dominated by stars older than several billion years. These objects range from dEs with $M_B \geq -18$ and total masses $\leq 10^{10}\,M_\odot$ down to dSphs with $M_B > -11$ and total masses $\geq 10^6 - 10^7\,M_\odot$. While the smallest dSphs have masses and luminosities comparable to massive star clusters, they are physically different entities. Dwarf galaxies sit inside the gravitational potential wells of dark matter halos, and the kinematics of their stars are increasingly dominated by this underlying dark matter halo (e.g. Aaronson 1983; but see Geha, Guthathakurta, & van der Marel 2002), whereas star clusters do not have associated dark matter halos (Pryor et al. 1989; Moore 1996). Massive globular clusters are compact, high-surface brightness objects, while dE/dSphs are diffuse and extended with decreasing surface-brightnesses with decreasing luminosities (Kormendy 1985). Most star clusters consist of a single population of stars with uniform age and chemical composition. On the other hand, studies of the color-magnitude diagrams and spectroscopic abundances of individual stars in Local Group dEs/dSphs show surprisingly complex star-formation and chemical enrichment histories in even the faintest galaxies (e.g. Carigi, Hernandez, & Gilmore 2002; Grebel 1997; Smecker-Hane et al. 1994).

The complex star-formation histories of the nearest dEs/dSphs are probably regulated by a number of mechanisms. Because of their low masses and shallow gravitational potential wells, dwarf galaxies are potentially fragile systems. The radiation, stellar winds, and supernovae produced by the first generations of stars can photo-dissociate, shock-heat, and expel much of the remaining gas, thereby suppressing future star-formation. Dekel and

Silk (1986) and later work by Dekel & Woo (2003) showed that the onset of supernovae-driven winds could explain the observed scaling relations of metallicity and mass-to-light ratio with total luminosity for galaxies less massive than $\sim 10^{10} M_\odot$. External heating by the high background of ultraviolet photons prevalent at early times in the universe (the epoch of re-ionization) can photo-ionize and even photo-evaporate small gaseous halos and prevent star-formation altogether (Efstathiou 1992; Babul & Rees 1992; Bullock, Kravtsov, & Weinberg 2000). Dwarf halos with virial velocities < 15 km s^{-1} which collapse after re-ionization may never accrete gas or form stars and remain dark (Bullock et al. 2000), while more massive halos and those which collapse prior to re-ionization in over-dense regions may produce some stars, albeit very inefficiently (Dong, Murray, & Lin 2003). Dwarf halos may also be rejuvenated by accreting new gas and/or cooling sufficiently to form stars after the UV-background has sufficiently cooled at $z \sim 1$ (Babul & Rees 1992, Efstathiou 1992). Finally, star-formation in dwarf galaxies may be strongly dependent on their environments and interactions with other galaxies. dEs are found exclusively as the satellites of massive galaxies or in rich clusters of galaxies. The rich cluster environment can ram-pressure strip accreted field dwarfs of their gas (Lin & Faber 1983) and transform or tidally destroy dwarfs via multiple encounters with more massive galaxies (Moore, Lake, & Katz 1998; Kravtsov, Gnedin, & Klypin 2004).

Disentangling the effects of these different processes on the evolution of dEs is challenging. In the Local Group, we have the advantage of proximity and can resolve the stars in ~ 20 dEs/dSphs. The color-magnitude diagrams and spectroscopic abundances of these stars can then be used to trace the star-formation and chemical enrichment histories of the dSph (eg. Grebel 1997). In the Virgo and Fornax Clusters are thousands of dEs, but because of their distances, current (largely ground-based) studies of these objects have been limited to the integrated colors and spectra. In this study of Leo, Virgo and Fornax Cluster dEs, we still cannot examine the properties of their individual stars. However, with HST resolution, we can distinguish their bright star clusters and nuclei from the stellar envelopes of field stars and use the colors of these three sub-populations to constrain the evolution of cluster dEs.

dEs and dSphs possess increasing globular cluster specific frequencies (number of globular clusters per host galaxy luminosity normalized to $M_V = -15$) at fainter luminosities (Miller et al. 1998). Studies of the globular cluster systems of Local Group dSph and a few dEs outside of the Local Group indicate that the majority of dE globulars are as old and metal-poor as the oldest globular clusters in the Milky Way ([Fe/H]< -1.0, >10 Gyr), and are significantly more metal-poor than their associated field star populations (Strader et al. 2003; Puzia et al. 2000; Buonanno et al. 1999; Da Costa & Mould 1998; Durrell et al. 1996a,b). A handful of intermediate-age and metal-rich clusters are also found in the Local

Group dSph (van den Bergh 2000). High-resolution numerical simulations of the collapse of dwarf-sized $10^8\,M_\odot$ dark matter halos predict the formation of dense $10^5\,M_\odot$ star clusters within dwarf halos at redshifts greater than 10 (Bromm & Clarke 2002). However, the origin of metal-poor globular clusters as "pre-galactic" (Peebles & Dicke 1968; Burgarella et al. 2001; Beasley et al. 2003) or associated with galaxy formation and assembly (Searle & Zinn 1978; Cote et al. 1998; Bromm & Clarke 2002; Kravtsov & Gnedin 2003) remains controversial.

Bright dEs often have luminous compact stellar nuclei. The nature and formation of the dE nuclei are poorly understood. The fraction of nucleated Virgo dEs increases with both dE luminosity (Binggeli & Cameron 1991) and position within the cluster (Ferguson & Sandage 1989). In dense environments such as the centers of clusters of galaxies, the pressure from the surrounding inter-galactic medium may allow dwarf galaxies to retain their gas during star formation and produce multiple generations of stars (Babul & Rees 1992), forming nuclei in the process. Spectroscopy of several bright Fornax dE nuclei show Balmer lines stronger than the metal-rich globular cluster 47 Tuc (Held & Mould 1994; Brodie & Huchra 1990), and NGC 205's nucleus is very blue and has strong Balmer line absorption (Jones et al. 1996; Ho, Filippenko, & Sargent 1995). These examples suggest that the stars in many dE nuclei may have formed quite recently. However, Sagittarius's probable nucleus is the massive, old, and metal-poor globular cluster M54 (Sarajedini & Layden 1995). The expected dynamical friction timescales for massive globular clusters in the low-density dEs is quite short, therefore many nuclei could simply be bright clusters that have spiraled into the center (Lotz et al. 2001; Oh & Lin 2000; Hernandez & Gilmore 1998), and contain predominately old and metal-poor stars.

The integrated colors and spectral features of the field stars in nearby cluster dEs are consistent with the intermediate and old mean ages ($\sim 4 - 13$ Gyr) and intermediate metallicities ($-1.0 < $ [Fe/H] < 0) derived for most Local Group dE/dSphs (e.g. Rakos et al. 2001; Conselice, Wyse, & Gallagher 2003; Geha et al. 2003). The details of the past star-formation events are impossible to recover from the integrated colors and spectral features of a complex stellar population; however spectroscopic measurements of the abundance of alpha elements (produced in both Type I and II SN) as compared to iron (primarily produced in Type I SN) give α/Fe ratios equal to the solar value and below (Thomas et al. 2003; Geha et al. 2003). This implies that the majority of stars in dEs were produced more than 1 Gyr after initial onset of star-formation and after Type I SN chemically-enriched the dE interstellar medium.

In this paper, we examine the $V - I$ colors of the globular clusters, nuclei, and field stars of 69 dwarf elliptical galaxies observed with the Hubble Space Telescope. In §2, we

describe our globular cluster detection and photometry, and the photometry for the dE stellar envelopes. In §3, we present the observed colors for each of these sub-populations and their dependence on the host galaxy properties and environment. In §4, we discuss the implications of the observed correlations for the formation of dE globular cluster systems and the star-formation histories of dEs.

2.   HST dE SNAPSHOT SURVEYS I, II, & III

The HST Dwarf Elliptical Galaxy Snapshot Survey has observed 69 dEs (Table 1) in the Leo Group and the Virgo and Fornax Clusters with the Hubble Space Telescope Wide Field/Planetary Camera 2 (HST WFPC2, GO Programs 6352, 7377, and 8500). The dE sample spans 6 magnitudes in M_B ($-12 < M_B < -18$) and has 45 nucleated and 24 non-nucleated dEs. HST WFPC2 images in filters F555W (2×230 s) and F814W (300 s) were taken of each galaxy, with the galaxy centered on chip WF3. The data were corrected for instrumental signatures by the standard HST calibration pipeline. A combined, cosmic-ray rejected F555W image was created with the cosmic-ray rejection routine COSMICRAYS (R. White, priv. comm.) and used as a template to identify and remove cosmic-rays from the single F814W image.

2.1.   Globular cluster candidate detection and photometry

Globular clusters are compact bright star clusters, with typical absolute magnitudes $-4 > M_V > -11$ and half-light radii $\sim 3 - 4$ pc (Ashman & Zepf 1998). The high angular resolution of the WFPC2 images ($\sim 0.1''$ per pixel) allows us to distinguish bright globular cluster candidates and nuclei from the underlying diffuse halo of dE field stars. At the distance of the Leo Group and the Virgo and Fornax Clusters, globular clusters are not truly resolved in short exposures by the WF camera and may be treated as point sources. The IRAF DAOPHOT point-source detection algorithm was run on the combined, cosmic-ray corrected F555W image to identify compact sources with fluxes 3σ above the background within a 0.2 $''$ radius aperture. The F555W and F814W fluxes for all detected point sources were measured within this aperture, and corrected for the missing flux in the wings of the PSF (i.e. aperture-corrected). The average aperture corrections for the WF chips are -0.275 ± 0.014 magnitudes for F555W and -0.307 ± 0.015 magnitudes for F814W (see §2.4 in Miller et al. 1997 for description of how these corrections are calculated). We also corrected the flux of the globular cluster candidates for the charge transfer efficiency effects across the WF chips (Whitmore & Heyer 1995). We adopted the Holtzman et al. (1995)

photometric calibrations to transform our F555W and F814W photometry to the standard Johnson V and Cousins I values. Foreground Galactic extinction and reddening values were taken from Schlegel et al. (1998, courtesy of the NASA Extragalactic Database) for each galaxy. Because most dEs are gas-poor systems, we assumed no internal extinction. Only FCC46 shows evidence for internal dust and active star-formation (Drinkwater et al. 2000). We adopted distance moduli of 30.0 for the Leo Group, 30.92 for the Virgo Cluster, and 31.39 for the Fornax Cluster, based on the Cepheid distances calculated by the HST Key Project (Freedman et al. 2001). It is important to note that these are average distances to these clusters and that the Virgo and Fornax Clusters have a depth along the line of sight of $\sim 1 - 2$ Mpc (Neilsen & Tsventanov 2000). We do not have independent distance estimates for each dE, and so the absolute magnitudes for the globular clusters and dEs have distant-dependent uncertainties on the order of ± 0.15 magnitudes.

Globular cluster candidates (GCCs) were selected based on size (FWHM$_{F555W} < 2.5$ pixels), $V - I$ color ($0.5 < V - I < 1.5$ and error $(V - I) < 0.3$), and proximity to the galaxy (see Miller et al. 1997 for discussion of globular cluster candidate color and size selection). Compact background galaxies and foreground stars within our color criteria may be mistaken for globular cluster candidates, and there may exist intergalactic globular clusters which are not bound to the dEs. We must correct for this contamination when estimating the number of globular clusters associated with each dE and examining their colors. In Tables 2 and 3, we have assumed that objects meeting our candidate criteria on WF chips 2 and 4 and outside of an elliptical aperture centered on the dE with semi-major axis length equal to 5 times the dE's exponential scalelength are background contaminants (Figure 1). The number density per area of these background objects were used to correct the number of observed GCCs on WF chip 3 and those on WF chips 2 and 4 that lie within 5 scalelengths of each dE.

Monte Carlo simulations of our point source detection indicate that our detections become incomplete at $V \sim 25.7$. Assuming that dE globular clusters have a intrinsic luminosity function similar to the Milky Way globular cluster luminosity function, we detect $\sim 85\%$ of the globular clusters in the Fornax dE images, 90% of the globular clusters in the Virgo dE images, and 98% of the globular clusters in the Leo dE images.

2.2. Galaxy photometry

The HST snapshot observations are not well suited to measuring the total galaxy luminosities. The flux of brightest dEs spills out onto chips WF2 and WF4, whereas the faintest (and lowest surface brightness) dEs are barely detectable above the sky noise. Stiavelli et

al. (2001) fit the surface brightness profiles for a subset of 25 dEs (observed during cycle 6) with Sersic profiles and derived total magnitudes from their fits. They also measured the color profiles and find little evidence for radial color gradients. Therefore the color measured within a fixed aperture should be a reliable estimate of the galaxy's true color.

We measured the relative fluxes of V and I within a fixed isophotal aperture for 45 dEs in our sample with central surface brightnesses $\mu_V < 24$ magnitudes per $\square''$, using the galaxy photometry package SExtractor (Bertin & Arnouts 1996). In order to improve the signal to noise for the galaxy detection algorithm, the F555W and F814W images were summed together and used as the SExtractor detection image. The isophotal aperture for each galaxy was set at 1σ above the sky level in the summed image; a lower detection threshold resulted in numerous spurious noise detections around the perimeter of the galaxy and a higher detection threshold failed to find the dEs. The galaxy flux within this aperture was then measured for the F555W and F814W images separately. SExtractor also corrects the measured galaxy fluxes for extended background galaxies observed directly behind the galaxy. The flux from the compact globular cluster candidates and the central nuclei was included in the isophotal flux of the galaxy. Most nuclei are too faint to contribute significantly to the measured colors of the dE stellar envelopes. The two brightest nuclei are the red nucleus of VCC1254 ($M_V = -12.25, V - I = 1.01$) and the very blue nucleus of FCC46 ($M_V = -12.16, V - I = 0.58$). For these two galaxies, we masked out the nuclei and re-measured the stellar envelope color. We found no change in the color of FCC46, while VCC1254 became 0.05 magnitudes redder. Given that the errors on the galaxy colors are ≥ 0.03, we expect that the rest of the nuclei will have a negligible effect on the dE halo colors.

The measured galaxy colors were transformed to the Johnson-Cousins photometric system using the same equations as the globular clusters (Holtzman et al. 1995). Due to the extended nature of the galaxies, no charge transfer efficiency corrections were applied to the galaxy colors. Ignoring this correction adds an additional $\leq 1.5\%$ uncertainty. The galaxy colors were de-reddened using the Schlegel et al. (1998) foreground extinction values. The galaxies' surface brightness profiles were measured from the WFCP2 F555W images in elliptical apertures using the IRAF task ELLIPSE and fit to exponential profiles:

$$I(r) = I_0 \exp(-r/r_0) \tag{1}$$

where I_0 is the central intensity and r_0 is the exponential scalelength.

3. COLORS OF dE STELLAR POPULATIONS

3.1. dE Globular Cluster Systems

Although dEs have large numbers of globular clusters for their luminosities (Miller et al. 1998), they are faint and possess at most a handful of clusters. We generally find less than 20 GCCs above the background counts for each dE (Tables 2 and 3). Because of the relatively high fraction of background contamination ($\sim 30 - 50\%$), determining the mean color and the color distribution for each dE globular cluster system is impossible without spectroscopic confirmation of the globular cluster candidates. Instead, we have constructed *composite* cluster color distributions for all the dEs within a given absolute magnitude range. By binning the globular cluster candidates by host galaxy luminosity, we improve our number statistics, can correct for the background contamination, and look for broad trends with dE luminosity.

A $V - I$ color histogram is created for all of the GCCs for the dEs within a luminosity range and normalized to the total area of the galaxies sampled (left of Figure 2). Then the $V - I$ color histogram for all background objects (also normalized to the total area of the background detections) is used to correct for the background object color distribution. The resulting background-corrected GCC color histograms are shown in heavy solid lines in the right of Figure 2. Also shown in Figure 2 are the color histograms produced by "bootstrapping" or re-sampling at random the original sample of background objects and dE GCCs 100 times (gray histograms) to illustrate the uncertainty of each derived color distribution. Each bootstrapped distribution contains the same number of background objects and dE GCCs as the original sample, but does not require that each replacement data point be unique.

Most of the dE GCCs are as blue in $V - I$ as the metal-poor globular clusters in the Milky Way and other bright galaxies (Harris 1991; Forbes & Forte 2000; Kundu & Whitmore 2001). We detect very few globular cluster candidates bluer than $0.6 - 0.7$. This is also consistent with the minimum globular cluster metallicity observed in the Milky Way ([Fe/H] ~ -2.5, Laird et al. 1988). Assuming the dE globular cluster candidates are as old as typical Milky Way globular clusters (≥ 10 Gyr), their color range agree with the metallicity range found for the globular cluster observed in Local Group dwarf spheroidal galaxies (dSphs) and nearby dEs ($-2.5 <$ [Fe/H]< -1.0; see Table 5).

However, the dE GCC color distributions are not uniform. We find that the GCC color distribution significantly broadens and the mean $V - I$ color becomes slightly redder with increasing dE luminosity (Figure 2). We have randomly re-sampled the original background objects and dE GCCs 10,000 times and fit single Gaussians to the binned and background-corrected color distributions with the IDL routine GAUSSFIT in order to derive peak $V - I$

colors and $\sigma(V - I)$. In Figure 2, we have plotted the Gaussian fits with the median peak color for the 10,000 bootstrapped color distributions (see also Table 4). This median color distribution has a peak $V - I = 0.83 \pm 0.02$ and $\sigma(V - I) = 0.03 \pm 0.01$ for the faintest dEs $(-11.7 < M_B < -13)$ and a peak $V - I = 0.90 \pm 0.01$ and $\sigma(V - I) = 0.13 \pm 0.01$ for the brightest dEs $(-16 < M_B < -17)$. We find that a linear fit to the observed peak GCC color - dE luminosity trend gives a shallow but significant slope :

$$\langle V - I \rangle_{GC} = -0.018(\pm 0.006) \times \mathrm{M_B}(\mathrm{dE}) + 0.606(\pm 0.093) \tag{2}$$

with $\bar{\chi}^2 = 0.46$.

In Figure 3, we compare the peak $V - I$ colors to the average colors of the literature dEs (Table 5), giant elliptical galaxy (E) and S0 globular cluster systems (Kundu & Whitmore 2001, Gebhardt & Kissler-Patig 1999; here after KW01 and GKP99). We have converted the literature values for the mean [Fe/H] of the globular cluster systems of five Local Group dE/dSphs, as well as three dEs outside of the Local Group, to a $V - I$ color with the empirical globular cluster $V - I$ - metallicity calibration of Kissler-Patig et al. (1998):

$$[\mathrm{Fe/H}] = -4.50 + 3.27(V - I) \tag{3}$$

(This conversion implicitly assumes that the globular clusters are relatively old.) The E/S0 globular cluster systems show a great deal of scatter in their mean colors, and the E/S0 sample spans a small range in luminosity, thus there has been some debate in the literature over the existence of a GC color - host galaxy luminosity trend (Harris 1991; Ashman & Zepf 1998; Strader, Brodie & Forbes 2004). However, for all but a few galaxies, the average colors of the E/S0 colors are consistent with the color-luminosity trend observed in dE sample, as are the 8 nearby dE/dSph GCS. Including the $V - I$ colors derived from the literature mean [Fe/H] values for dSph and dE, we find

$$\langle V - I \rangle_{GC} = -0.026(\pm 0.005) \times \mathrm{M_B}(\mathrm{dE/dSph}) + 0.491(\pm 0.079) \tag{4}$$

with $\bar{\chi}^2 = 0.93$. Including the 70 E/S0 $\langle V - I \rangle_{GC}$ colors from GKP99 and KW01 in our linear fit gives a worse $\bar{\chi}^2 = 3.31$ but a similar slope for the GC color - V-band luminosities:

$$\langle V - I \rangle_{GC} = -0.026(\pm 0.001) \times \mathrm{M_V}(\mathrm{dE/dSph/E/S0}) + 0.484(\pm 0.024). \tag{5}$$

The globular cluster color distributions are clearly broader for E/S0s than the dEs. In Figure 4, we illustrate the increasing breadth of the color distributions as a function of host galaxy luminosity. In both panels of Figure 4, the dE GCC peak colors are plotted as a function of dE M_V (assuming $M_V = M_B - 0.7$ where M_V is unavailable) and the Gaussian color dispersions $\sigma(V - I)$ given in Table 4 are shown as the error-bars. We have excluded

the literature dE/dSph GCS from these plots because of the small numbers of GCs in each system and the uncertainties associated with calculating a robust mean color and dispersion for very small samples (see Strader et al. 2004). In the top panel, we compare our dEs to the fitted $V - I$ color distributions for 43 E/S0 globular cluster systems taken from GKP99. They fit the $V - I$ color distributions with a bi-weight estimate of the location and scale, which correspond to a Gaussian mean and σ to first order. We have binned the E/S0 GCS by host galaxy luminosity, and plot the mean GKP99 peak $V - I$ values, with error-bars to indicate the mean scale (roughly equivalent to $\sigma(V - I)$), along side our dE globular cluster peak colors and $\sigma(V - I)$ (Figure 4) as a function of host galaxy luminosity. While the overwhelming majority of E/S0 globular cluster systems have $\sigma(V - I)$ larger than those observed in the brightest dE, there is no correlation between $\sigma(V - I)$ and E/S0 luminosity.

In the bottom panel of Figure 4, we plot the dE $\langle V - I \rangle_{GC}$ and $\sigma(V - I)$ with the results of bi-modal Gaussian fits to "red" and "blue" globular cluster peaks for 16 E/S0s (Larsen et al. 2001). The fitted peak colors for the E/S0 blue globular clusters are consistent with the extrapolation of the peak GC color- host galaxy luminosity trend observed in our sample of dEs (Equation 2), but are significantly bluer than the correlation derived when the literature dE/dSph cluster systems are included (Equation 4). Strader et al. (2004) also converted the metallicities of 9 dSph/dI globular clusters systems to $V - I$ color using a different relation and found that their colors were consistent with the color-luminosity dependence observed the blue GCs of ellipticals and spirals. While all galaxies possess globular clusters as blue as those in dEs, the brighter galaxies also possess increasing proportions of globular clusters redder than $V - I \sim 1.1$. The broadening in color distribution combined with the increasing number of the reddest globular clusters is what gives rise to the trend observed in Figure 2, rather than a shifting narrow distribution.

3.2. dE field stars

Early work on the Fornax dE population by Caldwell & Bothun (1987) found that dEs followed the $U - V$ vs. B color-magnitude relation observed for the Fornax giant ellipticals. However, dEs showed increased scatter in their colors and nucleated dEs were redder than non-nucleated dEs at the same luminosity. The observed color-magnitude slope was consistent with the metallicity-luminosity relation found for Local Group dSph ($Z \propto L^{0.4}$, Dekel & Silk 1986). Similar E/dE color-magnitude slopes have been subsequently observed in the Fornax (Cellone et al. 1994, Rakos & Schombert 2004), Coma (Secker & Harris 1996), and Perseus Clusters (Conselice et al. 2002), again with increased scatter towards the fainter luminosities. Spectroscopic abundances have confirmed that cluster dEs

and Local Group dSphs follow the metallicity-mass correlation of giant ellipticals (Geha et al. 2003; Thomas et al. 2003). However, several more recent studies of the Fornax Cluster dE/dSph populations which probed luminosities as faint as $M_V \sim -10$ have derived slightly shallower $V - I$ color v. V magnitude slopes that imply $Z \propto L^{0.3}$ (Hilker, Mieske, & Infante 2003; Karrick, Drinkwater, & Gregg 2003).

We find that the integrated dE field star populations are redder than their globular clusters by $0.1 - 0.2$ magnitudes (Figure 5). When we examine the nucleated dE and non-nucleated dEs separately, we find evidence for a color-luminosity trend for the nucleated dEs, whereas no such trend is evident for the non-nucleated dEs. A Spearman rank correlation test finds a 99.7 % probability of a color-luminosity correlation for nucleated dE, and a 44.8 % probability of correlation for non-nucleated dE. The entire dE sample gives a 94.6 % probability of a color-luminosity correlation. The derived color-magnitude relations are:

$$
\begin{aligned}
(V - I)_{FS} &= -0.031(\pm 0.010) \times M_B(\text{dE}) + 0.577(\pm 0.153) \quad \text{for dE, N only} \\
(V - I)_{FS} &= -0.014(\pm 0.005) \times M_B(\text{dE}) + 0.829(\pm 0.009) \quad \text{for all dE}
\end{aligned}
\tag{6}
$$

The slope of the color-magnitude relation for the dE,N matches the shallower trends found by Hilker et al. (2003) and Karrick et al. (2003), but is not inconsistent with the slightly steeper slope for cluster ellipticals. When both nucleated and non-nucleated dEs are considered, the color-magnitude relation has a slope more like than found for the globular cluster systems but with a higher zeropoint.

Several groups have claimed evidence for gradients in the color of dE population with distance from the cluster centers (Secker 1996; Rakos et al. 2001), which would imply age or metallicity dependence on cluster position. In Figure 6, we plot galaxy color as a function of projected distance from the (closest) central cluster galaxy (M51 for the Leo Group, NGC1399 for Fornax, and either M87 or NGC4472 for Virgo). We find no obvious correlation between dE stellar halo color and the projected radial distance from the central cluster galaxy for both the Virgo and Fornax cluster dEs ($p < 59\%$).

3.3. dE nuclei

We identify the nucleus of each dE,N galaxy as a bright compact object within 1.5 $''$ the dE's isophotal center. All nuclei meet our cluster candidate criterion (implying sizes < 10 pc), and are measured via the aperture photometry described in §2.2. We find 6 galaxies with previously unidentified nuclei (FCC46, FCC150, FCC242, FCC246, VCC646, and VCC1577). VCC9 was originally classified as nucleated by Binggeli et al. (1985), but its brightest globular cluster candidate is 1.8 $''$ from its center.

The dE nuclei are significantly bluer than their stellar envelopes (top left of Figure 7), contradicting previous ground-based studies (Caldwell & Bothun 1987; Rakos & Schombert 2004). Two dEs possess very blue nuclei with $V − I < 0.6$ (VCC1714 and FCC46). We find a correlation between nuclear color and dE color ($p = 98.9\%$), where redder nuclei are found in redder and brighter dEs and one of the bluest nuclei lies in a very blue dE (FCC46). Nuclear luminosity is a strong function of the host galaxy's luminosity, although with a ~ 1 magnitude dispersion not accounted for by the photometric uncertainties (top right of Figure 7).

The nuclei colors are also correlated with host galaxy luminosity at the 99.5% confidence level (bottom left of Figure 7), with a linear fit giving

$$(V − I)_{nucleus} = −0.031(\pm0.004) \times M_B(\text{dE}) + 0.487(\pm0.055) \tag{7}$$

When the two very blue nuclei are excluded, nuclear color is also found to be correlated with nuclear luminosity at the 99.5% level (bottom right of Figure 7), with a slope as shallow as for the nuclear color- host galaxy luminosity trend (bottom left of Figure 7).

The nuclei are often slightly redder than the dE globular cluster systems (bottom left of Figure 7). Many nuclei are much brighter than typical globular cluster candidates, which have a peak in their luminosity function at $M_V = −7.4$ (Miller 2003). Because nuclei become redder as they increase in luminosity, we have compared the faint ($M_V \leq −10$) nuclei colors to those of the dE globular cluster candidates with the same range of absolute magnitudes. We find no color difference between the dE nuclei and globular clusters at fixed nucleus/cluster luminosity, suggesting that the faint nuclei are indistinguishable from bright globular clusters.

We have also looked for trends in the dE nuclear properties with position in the Virgo and Fornax Clusters. As with the dE stellar envelopes, we fail to find any significant nuclear color or luminosity trends with distance from central cluster galaxy, even when the two very blue nuclei are excluded from the sample ($p < 49.2\%$; Figure 8).

4. DISCUSSION

4.1. Constraints on Ages and Metallicities

The integrated $V − I$ color of a stellar population is primarily a function of the temperature of the stellar population's red-giant branch, which becomes hotter and bluer with younger ages as well as lower metallicities. Therefore with a single optical color, it is impossible to distinguish between a young, metal-rich stellar population and an old, metal-poor

stellar population. Nevertheless, we attempt to place some reasonable constraints on the relative ages and metallicities for the dE stellar populations given the observed $V - I$ and what we know about local dE/dSph systems. Using the Bruzual & Charlot (2003) population synthesis models for a single starburst with a Salpeter stellar initial mass function and the Padova 1994 isochrones, we have plotted the range of possible ages and metallicities for the dE stellar halos ($0.9 < V - I < 1.15$) and dE globular clusters ($0.8 < V - I < 1.0$) in Figure 9. In these plots, the dashed lines are lines of constant $V - I$ color, and the shaded regions show the range of observed colors and possible ages and metallicities for each dE stellar population. Most of the dE stellar halos have $V - I > 0.95$ (Figure 6), implying luminosity-weighted ages > 2 Gyr and [Fe/H] > -1.6, consistent with the more precise ages and metallicities of dSph/dEs derived via spectroscopic absorption lines and resolved stellar color magnitude diagrams (Geha et al. 2003; see also Table 5). The bluer colors of the globular clusters (and nuclei) give much weaker constraints, but are consistent with [Fe/H] < -1.4 observed for old dSph GCs (Table 5). The Bruzual & Charlot (2003) tracks for the colors of the GCs in the faintest dEs ($V - I < 0.85$) imply that these clusters are younger than 8 Gyr. (However, the older Bruzual & Charlot models allow for ages greater than 8 Gyr if [Fe/H] < -1.7 and $0.8 < V - I < 0.85$. Also, several Milky Way globular clusters have integrated $V - I < 0.85$, $-1.4 >$[Fe/H] > -2.2, and ages ≥ 10 Gyr.) The model tracks also require that the two nuclei with $V - I < 0.6$ are younger than 1 Gyr.

The color offset between the dE stellar halos and their globular cluster systems requires that the bulk of the dE field stars are either significantly more metal-rich or older than their globular clusters. If the dE globular cluster systems were bluer because they were several Gyr younger than the dE field stars, one may expect them to be ~ 0.6 magnitudes brighter than old Milky Way globular clusters of the same mass and color. However, initial estimates of the composite dE globular cluster luminosity function (GCLF) indicate that its characteristic luminosity is identical to that of the Milky Way ($M_V = -7.4 \pm 0.1$; Miller 2003). Given that Local Group dE/dSph globular clusters systems are more metal-poor than their hosts' field stars and that the dE GCLF is indistinguishable from that of the Milky Way, we will assume that our sample of dE GCs is dominated by old and metal-poor globular clusters for the rest of this discussion. This implies either separate star-formation epochs for the dE GCs and field stars, or a strong metallicity gradient for dE stars with the destruction of the inner and more metal-rich clusters and the inward migration of the outer, more metal-poor clusters. Most dE nuclei span a similar color range as the dE GCs, and therefore could be coeval with the dE GCs. However, the existence of two very blue nuclei requires that some nuclei are formed in a later star-formation event, after both the dE globular cluster and field star formation epochs. In this section, we discuss the possible formation histories of these three dE sub-populations (clusters, field stars, and nuclei) and the constraints on the evolution of

the dEs.

4.2.   dE GC formation

The observed correlations between dE GC colors and host dE luminosities is strong evidence that the GCs knew about the gravitational potentials of their host dEs during their formation and were not accreted by the dEs at a later time. This rules out a primordial or pre-galactic origin for the globular clusters in dEs (Peebles & Dicke 1968). If the majority of the dE globular clusters are old and roughly coeval, the observed mean GCS color- host galaxy luminosity relation suggests a mean GCS metallicity - host galaxy luminosity correlation of

$$
\begin{aligned}
\langle Z \rangle_{GCS} &\propto L_B^{0.15\pm0.05} \quad \text{for our dEs only} \\
\langle Z \rangle_{GCS} &\propto L_B^{0.22\pm0.05} \quad \text{for all dSphs \&dEs} \\
\langle Z \rangle_{GCS} &\propto L_V^{0.21\pm0.02} \quad \text{for dSphs, dEs, \& E/S0s}
\end{aligned}
\tag{8}
$$

assuming the $(V-I)-$ [Fe/H] calibration of Kissler-Patig et al. 1998. The uncertainty in the color-metallicity calibration has been added to the errors in quadrature. If we assume the slighter steeper $(V-I)-$ [Fe/H] calibration for the Galactic globular clusters from Barmby et al. (2000), we find that the exponents for derived GC metallicity - host galaxy relations are 0.04 - 0.06 greater, but agree with those in Eqn. 8 to within the uncertainties. These correlations are significantly shallower than the metallicity-luminosity relation observed for the field star populations of local dwarf galaxies ($Z \propto L^{0.4}$, Dekel & Silk 1986), and that predicted for GCS by recent SPH hierarchical galaxy evolution models ($Z_{GC} \propto M_*^{0.5}$, Kravtsov & Gnedin 2003).

Assuming the dE GCs are older than 5 Gyr, the observed increasing color dispersion also implies an increasing dispersion in metallicity. The Simple model of galactic chemical evolution is the zeroth order model against which to compare the metallicity (and color) distribution of a stellar population (Tinsley 1975), or, because each globular cluster is a chemically homogeneous population, the metallicity distribution of a system of globular clusters. The Simple model assumes that 1) the galaxy is a "closed box" with no inflow or outflow of gas; 2) the metals are well mixed; 3) the galaxy is initially pure gas with primordial abundances; and 4) the nucleo-synthetic yields of stars are constant for "primary elements" (elements created directly from hydrogen and helium). The metallicity distribution of stars s for a Simple model is

$$
\frac{ds}{d\log(z)} \propto z \exp(-z)
\tag{9}
$$

where $z = Z/p$ and p is the effective chemical yield. In Figure 10, we have fit Simple model metallicity distributions to the $V-I$ color distributions, again assuming the Kissler-Patig

et al. (1998) color-metallicity calibration. (Strictly speaking, the Simple model distribution applies only to primary elements which follow the instantaneous recycling approximation, but may be applied to iron (Fe) if we assume the ratio of primary elements to Fe is constant). The background-corrected GC color distributions for the entire sample of dE GCC are well-fit by the Simple model, as are the GCC distributions for dEs brighter than $M_B = -15$, with effective yields $p \sim 10^{-1.5} Z_\odot$ ($\bar{\chi}^2 = 0.58 - 1.38$) The Simple model does poorly for fainter dEs ($M_B > -15$), although the numbers are small.

The comparison of the implied metallicity distributions of the dE globular cluster systems to Simple closed-box chemical evolution models suggests that a significant amount of metals is lost or unavailable for star-formation during the period of globular cluster formation. In closed systems, the effective yield is expected to reach the true chemical yield of supernovae. The low effective yield may be the result of a homogeneous wind, where gas and metals are lost proportionally to the star formation rate (Hartwick 1976). Fainter, less massive dEs would be more likely to experience a terminal wind in which all of the galaxy's gas is expelled at a particular time (for example, via supernovae "blow-out"; Arimoto & Yoshii 1987), and results in a sharp cutoff at higher cluster metallicities. For such cases where the gas is removed on very short timescales, the steep metallicity-luminosity scaling relation observed for the stellar halos of Local Group dSphs is expected ($Z \propto L^{0.4}$; Dekel & Silk 1986). We are unable to conclusively determine whether the field star colors of our dEs are more consistent with a $Z \propto L^{0.4}$ and $Z \propto L^{0.2}$ correlation because of the large scatter in the dE color-magnitude relation.

If the implied correlation between globular cluster metallicity and dE host galaxy luminosity is confirmed by more reliable metallicity estimates, and if the metallicity- luminosity relation of the dE field stars is like that of the Local Group dEs/dSphs, then the gas heating mechanism or timescales regulating the chemical evolution of dE globular clusters must be markedly different from that regulating the chemical evolution of dE field stars. We note that for slower adiabatic winds where the gas is removed on timescales comparable to the crossing time of the system, a metallicity - host galaxy luminosity scaling relation similar to that observed for the globular cluster systems is derived ($Z \propto L^{0.25}$; Dekel & Silk 1986). The GC formation model of Kravtsov & Gnedin (2003), which predicts too strong of a GC metallicity-host galaxy luminosity relationship, produces GCs during and after re-ionization in relatively massive halos ($M_{halo} > 10^9 M_\odot$). Smaller halos, however, may be unable to efficiently cool and form the dense molecular clouds needed for GC production after re-ionization and/or the on-set of supernovae-driven winds. GC formation in dwarfs prior to re-ionization would not be subject to the heating effects of a high UV-background, and therefore dwarf halos may initially lose metals more gradually than at later times.

It is impossible to determine from the $V - I$ colors alone if dE globular clusters were formed before or after the epoch of re-ionization. Globular clusters formed before re-ionization at redshifts ≥ 7 would be ~ 13 Gyr old, while clusters formed after the inter-galactic UV background had cooled at redshift ~ 1 would be ~ 8 Gyr old. One possible way to distinguish between these two formation epochs is to examine the chemical abun-dance patterns in dE globular clusters. Globular clusters do not have primordial abundances, therefore at least some stars must have formed and enriched the gas in dEs before the glob-ular clusters were produced. Chemical enrichment of the stellar halo would happen quite quickly, as massive stars have lifetimes less than 10^7 years. Assuming stars in the early universe evolve with the same timescales and nuclear processes as stars formed at later times (Qian & Wassberburg 2002), stars in dEs formed before the epoch of re-ionization would show enrichment patterns enhanced in α elements (relative to the Sun) created by massive, short-lived stars, as there would not be enough time prior to re-ionization for lower mass, primarily iron-producing stars to enrich the interstellar medium. The α-element abundance ratios of dE globular clusters are unknown, but spectroscopic observations of a small number of dEs suggest that their field stars are *not* alpha-element enhanced (Thomas et al. 2003; Geha et al. 2003), and therefore the majority of dE stars did not form prior to re-ionization.

Another possibility is that the dE field stars and globular clusters did not form in separate events, but rather a combination of strong metallicity gradients in the globular cluster populations and the preferential destruction of clusters with higher metallicities has produced the metallicity offset observed today. This might arise naturally if inner, more metal-rich clusters were destroyed via disk-shocking or dynamical decay into the dE centers, while outer, more metal-poor clusters migrated inwards. However, destruction of more metal-rich clusters via dynamical friction would produce dE nuclei with colors more like the dE field stars, which is not observed. Also, there is little evidence for strong metallicity gradients between the inner and outer regions of dE. Most dE show either no color gradients or bluer centers (Stiavelli et al. 2001; Jerjen, Binggeli, & Freeman 2000). Spectroscopic estimates of any abundance gradients in the dE field star populations as well as the α-element ratios of dE GCs would help resolve this issue.

4.3. dE Field Star Formation

The $V - I$ colors of the dEs are $0.1 - 0.2$ magnitudes redder than their globular clusters, and therefore the majority of the dE field stars probably did not form in the same event as their globular clusters. The majority of dE stars cannot be the remnants of a disrupted GC population (Fall & Rees 1977), nor were the Virgo and Fornax dE stellar populations formed

in a single starburst (e.g. Dekel & Silk 1986). Given the ages and metallicities derived for nearby dSphs/dEs and their GCs, it is most likely that the dE stars are more metal-rich, and possibly several Gyr younger than their GCS. An offset in metallicity suggests that the bulk of dE stars were formed after a period of ISM chemical enrichment, perhaps by the massive stars in the GCs. The initial epoch of globular cluster formation must have input a significant amount of energy into the dwarf's remaining gas in the form of UV radiation and supernovae-driven winds, as would background UV radiation during the epoch of re-ionization (e.g. Babul & Rees 1992, Efstathiou 1992). While the feedback from young clusters and a strong UV-background could have halted star-formation temporarily, it must not have been enough to completely "blow-away" or "photo-evaporate" the remaining gas, and therefore later generations of stars could have formed in the halo once the gas had cooled sufficiently. The observed solar and sub-solar α-element ratios in the dE stellar halos (Geha et al. 2003; Thomas et al. 2003) require field star-formation during or after a period of extended chemical enrichment, implying either a > 1 Gyr age difference between the dE field stars and their GCs or a > 1 Gyr age spread in the dE field stars. As we discussed above, the difference between the metallicity-host galaxy luminosity relations observed for the dE GCs and field stars suggests that different mechanisms regulated the chemical enrichment during each star-formation episode. Later star-formation events must have been much less efficient at forming massive, tightly bound GCs which could survive to present-day. (Only a few intermediate-age GCs have been found in Local Group dSph; van den Bergh 2000.) The different star-formation regulating mechanisms may have also lowered the star-formation efficiency below that required to create gravitationally-bound clusters (Kroupa et al. 2001).

We find evidence for a marginally significant color-luminosity trend in the dE,N that is not detected in dEs without nuclei. The non-nucleated dEs also have slightly bluer $V - I$ colors. This is suggestive of younger ages for the non-nucleated dE, although spectroscopically derived ages for a larger sample will be needed to confirm this. We find no clear environmental dependence on the dEs and dE,Ns colors (Figure 7). Other authors have found marginal trends for redder colors with larger projected cluster distances with ground-based data (Rakos et al. 2001; Secker 1996). A lack of correlation between dE color and cluster position would rule out the popular "infall" model for the origin of cluster dEs (Moore, Lake, & Katz 1998; Conselice et al. 2003), unless a age-metallicity conspiracy existed in which the dEs in the outskirts of clusters were both younger and more metal-rich than inner dEs.

4.4.   dE Nuclei Formation

The nuclei of dEs are significantly bluer than their associated stellar halos, unlike the nuclei and bulges of spirals and giant ellipticals. The nuclei have colors similar to the globular cluster systems and are as compact as the globular cluster candidates. They could possess some of the oldest stars in dEs, formed first in the densest regions of the dwarf halos or from the infall of massive globular clusters into the dE centers via dynamical friction (Lotz et al. 2001, Oh & Lin 2001, Hernandez & Gilmore 1998). Both nuclear formation scenarios are consistent with the correlations of nuclear color and luminosity with host galaxy luminosity. Brighter dEs have deeper central potential wells, and thus would be better able to accrete and retain gas to form brighter and more metal-rich nuclei. Brighter dEs also have redder and larger globular cluster populations from which their nuclei could coalesce.

Two dEs possess very blue nuclei which require ages < 2 Gyr, as does NGC 205, a dE satellite of M31 (Jones et al. 1996). If many nuclei are relatively young compared to typical globular clusters, they could trace a third star-formation episode, after both the globular cluster and dE halo formation events. The trend of bluer nuclei in fainter dE hosts might then imply that the nuclei in fainter dEs are typically younger than the nuclei in brighter dEs. However, the two very blue nuclei are in dEs brighter than $M_B = -15.8$. Spectroscopic line indices are needed to place stronger constraints on the ages, metallicities, and formation scenarios for the dE nuclei.

We find no significant trends for nuclear color or luminosity with local environment (Figure 8), nor do we find any significant differences between the Virgo and Fornax dE nuclei. This is contrary to the IGM pressure-induced star-formation model of Babul & Rees (1992), which predicts that nuclei formed in the densest regions of the cluster undergo the most intense and rapid starbursts and should be significantly older, more metal-rich and redder than dE nuclei formed in the outskirts of the cluster. This also contradicts the infall model for dE formation, in which nucleated dEs are the stripped remnants of disk galaxies that experience a central starburst upon accretion (Moore, Lake, & Katz 1998). Conversely, the nuclei are typically bluer and fainter than the ultra-compact galaxies observed in the Fornax Cluster with $-12 < M_V < -14$ (Karrick et al. 2003). While it seems unlikely that the ultra-compact galaxies have been drawn from the present-day dE,N population, perhaps the ultra-compacts are consistent with a tidally-disrupted population of spirals.

5. SUMMARY

We have examined the HST WFPC2 $V-I$ colors for the globular cluster systems, nuclei, and stellar envelopes of 69 dwarf elliptical galaxies in the Leo Group and Virgo and Fornax Clusters. We find the following:

(1) The mean and dispersion in GC $V - I$ color is a function of host dE luminosity. Assuming the majority of dE GCs are as old as Local Group dSph GCs, the implied metallicity-luminosity relation is $\langle Z_{GC} \rangle \propto L^{(0.15-0.22)}$, which is significantly shallower than that observed for the field stars of Local Group dSph ($\langle Z_{FS} \rangle \propto L^{0.4}$).

(2) The $\langle V - I \rangle_{GC}$ and host galaxy luminosities of E/S0s are consistent with the slope computed for our dE sample plus literature values for 8 local dE/dSph GCS. However, the E/S0 GCS color distributions often have a bi-modality not observed in dEs and show no correlation between $\sigma(V - I)$ and galaxy luminosity. The dE GCs are as blue as the metal-poor GC sub-populations observed in the Milky Way and local E/S0s. The blue GC peak color - host galaxy luminosity trend for E/S0 reported by Larsen et al. (2001) is consistent with the slope fit to the peak GC colors for our sample of dEs, but is shallower than the slope fit to our sample and literature dE/dSph GC values.

(3) With the exception of two very blue nuclei, the dE nuclei have colors similar to but slightly redder than the GCs, and show the same correlations with host galaxy luminosity. Their colors are also correlated with host galaxy color, as well as with nuclear luminosity.

(4) We measure the integrated $V - I$ colors for 45 dEs brighter than $M_B = -12.7$. The dE field stars are $0.1 - 0.2$ magnitudes redder than their GCs and nuclei, implying a more metal-rich stellar population. The colors of the nucleated dEs are weakly correlated with their luminosity, while the non-nucleated dEs show no significant correlation.

(5) We find no correlation between dE field star color or nuclear color and the dE's projected distance from the brightest cluster galaxy, nor do we find any significant difference between the colors of the Virgo and Fornax dE stellar populations.

Therefore, we conclude that:

(1) Virgo and Fornax Cluster dEs have probably undergone multiple star-formation episodes. Given the spectroscopic metallicities of Local Group dEs/dSphs, it is most likely that the redder dE field star populations are significantly more metal-rich and possibly younger than their associated GCs. At least two dE nuclei trace a third star-formation event less than 1 Gyr ago, after both the GC and field star formation epochs.

(2) dE GCs must have formed within the gravitational potential wells of proto-dE halos,

and were not produced in "pre-galactic" gas clouds.

(3) Assuming dE field star populations follow the same metallicity-luminosity relation as Local Group dEs/dSphs, the mechanisms regulating the chemical evolution of dE GCs are significantly different from that of the dE field stars. We suggest that the majority of dE GCs formed at early times, prior to re-ionization and/or strong feedback from supernovae, and therefore lost metals more gradually than stellar populations formed at later times. Subsequent star-formation events (after re-ionization and/or the onset of supernovae-driven winds) were subject to more rapid metal-loss and are unable to proceed as efficiently as needed to produce significant numbers of GCs.

(4) Cluster dE evolution models which predict strong color gradients with projected cluster radius for stellar envelopes and nuclei are ruled out. This includes both the infall model (Moore, Lake, & Katz 1998) and IGM pressure-induced star-formation scenario (Babul & Rees 1992).

REFERENCES

Aaronson, M. 1983, ApJ, 266, L11

Arimoto, N., & Yoshii, Y. 1987, A&A, 173, 23

Ashman, K.M. & Zepf, S.E. 1998, *Globular Cluster Systems* (Cambridge, U.K.: Cambridge University Press)

Babul, A. & Rees, M. 1992, MNRAS, 255, 346

Barmby, P., Huchra, J.P., Brodie, J.P., Forbes, D.A., Schroder, L.L., & Grillmair, C.J. 2000, AJ, 119, 727

Beasley, M.A., Kawata, D., Pearce, F.R., Forbes, D. & Gibson, B.K. 2003, ApJ, 596L, 187

Bertin, E., & Arnouts, S. 1996, A&AS,. 117, 393

Binggeli, B. & Cameron, L.M. 1991, A&A, 252, 27

Binggeli, B., Sandage, A., & Tammann, G.A. 1985, AJ, 90, 1681

Brodie, J.P., & Huchra, J. 1990, ApJ, 362, 503

Bromm, V., & Clarke, C.J. 2002, ApJ, 566, L1

Bruzual, G., & Charlot, S. 2003, MNRAS, 344, 1000

Buonanno, R., Corsi, C.E., Castellani, M., Marconi, G., Fusi Pecci, F., & Zinn, R. 1999, AJ, 118, 1671

Bullock, J.S., Kravtsov, A.V., & Weinberg, D.H. 2000, ApJ, 539, 517

Burgarella, D., Kissler-Patig, M., & Buat, V. 2001, AJ, 121, 2647

Caldwell, N., & Bothun, G.D. 1987, AJ, 94, 1126

Carigi, L., Hernandez, X. & Gilmore, G. 2002, MNRAS, 334, 117

Cellone, S.A., Forte, J.C., & Geisler, D. 1994, ApJS, 93, 397

Conselice, C.J.,Gallagher, J.S., & Wyse, R.F.G. 2002, AJ, 123

Conselice, C.J., Gallagher, J.S., & Wyse, R.F.G. 2003, ApJ, 125, 66

Côté, P, Marzke, R. O., West, M. J. 1998, ApJ, 501, 554

Da Costa, G.S., & Mould, J.R. 1988, ApJ, 334, 159

Dekel, A., & Woo, J. 2003, MNRAS, 344, 1131

Dekel, A. & Silk, J. 1986, ApJ, 303, 39

Dong, S., & Murray, S.D., Lin, D.C. 2003, ApJ, 596, 930

Drinkwater, M. J., Jones, J. B., Gregg, M. D., & Phillipps, S. 2000, PASA, 17, 227

Durrell, P.R., McLaughlin, D. E., Harris, W. E., & Hanes, D. A. 1996a, ApJ, 463, 543

Durrell, P. R., Harris, W.E., Geisler, D., & Pudritz, R.E. 1996b, AJ, 112, 972

Efstathiou, G. 1992, MNRAS, 256, 43

Fall, S.M. & Rees, M.J. 1977, MNRAS, 181, 37

Ferguson, H.C., & Sandage, A. 1989, ApJ, 346, L53

Ferguson, H.C., & Sandage, A. 1990, AJ, 100, 1

Forbes, D. & Forte J. 2001, MNRAS, 322, 257

Freedman, W.L. et al. 2001, ApJ, 553, 47

Gebhardt, K. & Kissler-Patig, M. 1999, AJ, 118, 1526

Geha, M., P. Guhathakurta, & R.P. van der Marel 2002, AJ, 124, 3073

Geha, M., P. Guhathakurta, & R.P. van der Marel 2003, AJ, 126, 1794

Geisler, D., Armandroff, T., Da Costa, G., Lee, M.G., & Sarajedini, A. 1999, in *The Stellar Content of Local Group Galaxies*, p. 231

Grebel, E. 1997, Rev. Mod. Astron., 10, 29

Han, M., Hoessel, J.G., Gallagher, J.S., Holtzman, J., & Stetson, P.B. 1997, AJ, 113, 1001

Harris, W. 1991, ARA&A, 29, 543

Hartwick, F.D.A. 1976, ApJ, 209, 418

Held, E.V., & Mould, J. 1994, AJ, 107, 1307

Hernandez, X., & Gilmore, G. 1998, MNRAS, 297, 517

Hilker, M., Mieske, S. & Infante, L. 2003, A&A, 397, L9

Ho, L., Filippenko, A.V., & Sargent, W.L. 1995, ApJS, 98, 477

Holtzman, J. A., Burrows, C. J., Casertano, S., Hester, J. J., Trauger, J. T., Watson, A. M., & Worthey, G. 1995, PASP, 107, 1065

Jerjen, H., Binggeli, B. & Freeman, K.C. 2000, AJ, 119

Jones, H., et al., 1996, ApJ, 466, 742

Karrick, A.M., Drinkwater, M.J., & Gregg, M.D. 2003, MNRAS, 344, 188

Kauffmann, G., White, S.D.M., & Guiderdoni, B. 1993, MNRAS, 264, 201

Kissler-Patig, M., Brodie, J.P., Schroder, L.L., Forbes, D.A., Grillmair, C.J., & Huchra, J.P. 1998, AJ, 115, 105

Kormendy, J. 1985, ApJ, 295, 73

Kravtsov, A.V., & Gnedin, O.Y. 2003, astroph/0305199

Kravtsov, A.V., Gnedin, O.Y., & Klypin, A.A., 2004, astroph/0401088

Kroupa, P., Aaresht, S., & Hurley, J. 2001, MNRAS, 321, 699

Kundu, A., & Whitmore, B.C. 2001, AJ, 121, 2950

Laird, J.B., Rupen, M., Carney, B., & Latham, D.W. 1988, AJ, 96, 1908

Larsen, S.S., Brodie, J., Huchra, J.P., Forbes, D.A., & Grillmair, C. 2001, AJ, 121, 2974

Lin, D.N.C. & Faber, S.M. 1983, ApJ, 266, 21

Lotz, J., Telford, R., Ferguson, H. C., Miller, B. W., Stiavelli, M., & Mack, J. 2001, ApJ, 552, 572

Martinez-Delgrado, D., & Aparicio, A., 1998, AJ, 115, 1462

Mateo, M. 1998 ARA&A, 36, 435

Miller, B.W. 2003, *Extragalactic Globular Cluster Systems*, 199

Miller, B.W., Lotz, J.M., Ferguson, H.C., Stiavelli, M., & Whitmore, B.C. 1998, ApJ, 508, L133

Miller, B.W., Whitmore, B. C., Schweizer, F., & Fall, S. M. 1997, AJ, 114, 2381

Monaco, L., Ferraro, F.R., Bellazzini, M., & Pancino, E. 2002, ApJ, 578, 47

Moore, B. 1996, ApJ, 461, 13

Moore, B., Lake, G., & Katz, N. 1998, ApJ, 495, 139

Montegriffo, P., Bellazzini, M., Ferraro, F.R., Martins, D., Sarajedini, A., & Fusi Pecci, F. 1998, MNRAS, 294, 315

Mould, J., Kristian, J., & Da Costa, G.S. 1984, ApJ, 278, 575

Neilsen, E. & Tsventanov, Z. 2000, ApJ, 536, 255

Oh, K.S., & Lin, D.N.C. 2000, ApJ, 543, 620

Peebles, P. J. E., & Dicke, R. H. 1968, ApJ, 154, 891

Pont, F., Zinn, R., Gallart, C., Hardy, E., & Winnick, R. 2004, AJ, 127, 840

Pryor, C., McClure, R.D., Fletcher, J.M, & Hesser, J.E. 1989, AJ, 98, 596

Puzia, T.H., Kissler-Patig, M., Brodie, J., & Schroder, L. 2000, A&A, 120, 1160

Qian, Y.-Z., & Wasserburg, Y. 2002, ApJ, 567, 515

Rakos, K., Schombert, J., Maitzen H.M., Prugovecki, S., & Odell, A. 2001, AJ, 121, 1974

Rakos, K., & Schombert, J., 2004, AJ, 127, 1502

Reaves, G. 1983, ApJS, 53, 375

Sarajedini, A., & Layden, A.C 1995, AJ, 109, 1086

Searle, L., & Zinn, R. 1978, ApJ, 225, 357

Secker, J. 1996, ApJ, 469L, 81

Secker, J., & Harris, W.E. 1996, ApJ, 469, 623

Schlegel, D. J., Finkbeiner, D. P., & Davis, M. 1998, ApJ, 500, 525

Smecker-Hane, T.A., Stetson, P., Hesser, J.E., & Lehnert, M.D. 1994, AJ, 108, 507

Stiavelli, M., Miller, B. W., Ferguson, H. C., Mack, J., Whitmore, B. C., & Lotz, J. M.2001, AJ, 121, 1385

Strader, J., Brodie, J.P., Forbes, D.A., Beasley, M.A., & Huchra, J.P. 2003, AJ, 125, 1291

Strader, J., Brodie, J.P., & Forbes, D.A. 2004, astro-ph/0403160

Thomas, D., Bender, R., Hopp, U., Maraston, C., & Greggio, L. 2003, Ap&SS,. 284, 599

Tinsley, B.M. 1975, ApJ, 159, 162

Tully, R.B., Sommerville, R.S., Trentham, N., & Verheijen, M.A. 2002, ApJ, 569, 573

van den Bergh, S. 2000, ApJ, 530, 777

Whitmore, B.C. & Heyer, I 1995, in *Calibrating Hubble Space Telescope. Post Servicing Mission.* eds. A. Koratkar, & C. Leitherer, Baltimore, Maryland: Space Telescope Science Institute, p. 305

Table 1.   HST dE Snapshot Survey I, II, & III

Galaxy[1]	IDs[2]	B[1]	M_B[3]	Type[1]	RA(J2000)	DEC(J2000)	A_V[4]	E_{VI}[4]
LGC47	UGC05944	15.2	−15.1	dE	10:50:18	13:16:19	0.093	0.039
LGC50	· · ·	17.0	−13.3	dEN	10:51:01	13:20:02	0.093	0.039
FCC25	NG31	17.7	−13.7	dE0N	3:23:33	−36:58:57	0.069	0.029
FCC27	· · ·	19.3	−12.1	dE2	3:23:56	−34:12:29	0.035	0.014
FCC46	· · ·	15.6	−15.8	dE4	3:26:25	−37.53:20	0.061	0.025
FCC48	NG61	17.1	−14.3	dE3	3:26:42	−34:28:04	0.036	0.015
FCC59	· · ·	19.4	−12.0	dE0N	3:27:47	−33:27:10	0.043	0.018
FCC64	· · ·	17.5	−13.9	dE5	3:38:00	−38:28:47	0.061	0.025
FCC110	NG26, ESO358-G14	16.8	−14.6	dE4	3:32:57	−35:16:44	0.050	0.021
FCC136	NG24	14.8	−16.6	dE2N	3:34:29	−35:28:11	0.053	0.022
FCC144	· · ·	19.2	−12.2	dE0	3:35:00	−35:41:39	0.047	0.020
FCC146	· · ·	19.5	−11.9	dE4N	3:35:31	−35:41:37	0.049	0.021
FCC150	· · ·	15.7	−15.7	dE4	3:35:24	−36:39:10	0.046	0.019
FCC174	· · ·	16.7	−14.7	dE1N	3:36:45	−33:00:10	0.026	0.011
FCC189	· · ·	18.8	−12.6	dE4N	3:37:08	−34:17:08	0.046	0.019
FCC212	NG119	17.6	−13.8	dE1?	3:38:21	−36:36:12	0.036	0.015
FCC218	NG72	18.5	−12.9	dE4	3:38:45	−35:41:31	0.041	0.017
FCC238	NG109	18.7	−12.7	dE5N	3:40:17	−36:28:54	0.031	0.013
FCC242	NG51	17.8	−13.6	dE5	3:40:20	−37:22:21	0.047	0.020
FCC246	· · ·	19.1	−12.3	dE2	3:40:37	−36:53:43	0.038	0.016
FCC254	NG22	17.6	−13.8	dE0N	3:41:00	−35:16:26	0.034	0.014
FCC304	· · ·	18.8	−12.6	dE1	3:45:30	−34:30:39	0.023	0.010
FCC316	NG12	16.7	−14.7	dE1N	3:36:45	−33:00:10	0.036	0.015
FCC324	ESO358-G66	15.3	−16.1	dS01(8)	3:47:52	−36:32:41	0.032	0.013
VCC9	IC3019, UGC07136	13.9	−17.0	dE1N	12:09:22	13:59:34	0.128	0.053
VCC118	R92	15.6	−15.3	dE3	12:14:36	9:41:20	0.053	0.022
VCC128	UGCA275, R903	15.6	−15.3	dE0	12:14:59	9:33:54	0.051	0.022
VCC158	UGC07269, R1513	15.8	−15.1	dE3N	12:15:40	15:00:18	0.131	0.055
VCC240	R1419	18.2	−12.7	dE2N	12:17:31	14:21:21	0.108	0.045
VCC452	R1223	15.8	−15.1	dE4N	12:21:04	11:45:18	0.093	0.039
VCC503	R817	16.8	−14.1	dE3N	12:21:50	8:32:31	0.062	0.026
VCC529	R1015	18.2	−12.7	dE4N	12:22:08	9:53:41	0.079	0.033
VCC543	UGC07436	14.8	−16.1	dE5	12:22:19	14:45:38	0.105	0.045
VCC546	R1017	15.7	−15.2	dE6	12:22:21	10:36:06	0.121	0.050
VCC646	· · ·	18.8	−12.1	dE3	12:23:31	17:47:42	0.099	0.041
VCC747	R924	16.2	−14.7	dE0N	12:24:47	8:59:21	0.072	0.030
VCC871	R1240	15.4	−15.5	dE4N	12:26:05	12:33:33	0.109	0.045
VCC896	R1352	17.8	−13.1	dE3N	12:26:22	12:47:03	0.096	0.040
VCC917	IC3344	14.9	−16.0	dE6	12:26:32	13:34:44	0.107	0.045
VCC940	IC3349, R1243	14.8	−16.1	dE1N	12:26:47	12:27:12	0.101	0.042

Table 1—Continued

Galaxy[1]	IDs[2]	B^1	$M_B{}^3$	Type[1]	RA(J2000)	DEC(J2000)	$A_V{}^4$	$E_{VI}{}^4$
VCC949	R1027	15.1	−15.8	dE4N	12:26:54	10:39:56	0.102	0.042
VCC965	IC3363, R1245	15.4	−15.5	dE7N	12:27:03	12:33:37	0.100	0.042
VCC992	R827	15.8	−15.1	dE0N	12:27:18	8:12:45	0.075	0.031
VCC996	R1360	18.4	−12.5	dE5	12:27:21	13:06:41	0.100	0.041
VCC1073	IC794, UGC07585	14.2	−16.7	dE3N	12:28:08	12:05:34	0.091	0.038
VCC1077	$\cdots$	19.2	−11.7	dE0N	12:28:09	12:48:23	0.078	0.032
VCC1105	R1440	16.2	−14.7	dE0N	12:28:27	14:09:15	0.146	0.061
VCC1107	NGC4472 DW01, R731	15.1	−15.8	dE4N	12:28:30	7:19:28	0.069	0.029
VCC1252	$\cdots$	18.8	−12.1	dE0N	12:30:01	9:28:24	0.066	0.028
VCC1254	NGC4472 DW08, R834	15.0	−15.9	dE0N	12:30:05	8:04:22	0.074	0.031
VCC1272	$\cdots$	18.5	−12.4	dE1N	12:30:15	13:18:28	0.088	0.036
VCC1308	IC3437	15.1	−15.8	dE6N	12:30:46	11:20:33	0.116	0.048
VCC1311	NGC4472 DW03, R737	15.6	−15.3	dE1N	12:30:47	7:36:18	0.063	0.026
VCC1363	$\cdots$	19.0	−11.9	dE3N	12:31:27	10:56:07	0.107	0.044
VCC1386	IC3457, UGC3457, R1264	14.4	−16.5	dE3N	12:31:51	12:39:42	0.084	0.035
VCC1497	UGC07707	15.7	−15.2	dE4N	12:33:18	17:27:35	0.086	0.036
VCC1514	$\cdots$	15.1	−15.8	dE7N	12:33:37	7:52:14	0.064	0.026
VCC1530	$\cdots$	18.3	−12.6	dE2N	12:33:55	5:43:07	0.075	0.031
VCC1577	IC3519, R1555	15.8	−15.1	dE4	12:34:38	15:36:10	0.093	0.038
VCC1651	R640	17.0	−13.9	dE5	12:36:07	6:03:10	0.063	0.026
VCC1714	R1461	18.5	−12.4	dE4N	12:37:25	14:18:46	0.097	0.040
VCC1729	$\cdots$	17.8	−13.1	dE5?	12:37:46	10:59:07	0.077	0.032
VCC1762	R1055	16.2	−14.7	dE6	12:38:32	10:22:37	0.072	0.030
VCC1781	R842	18.7	−12.2	dE4	12:39:11	8:04:17	0.087	0.036
VCC1876	IC3658, R1465	14.9	−16.0	dE5N	12:41:20	14:42:03	0.103	0.043
VCC1877	R844	18.6	−12.3	dE2	12:41:23	8:22:00	0.093	0.038
VCC1948	R1062	15.1	−15.8	dE3	12:42:58	10:40:54	0.080	0.033
VCC2008	IC3720, DDO145	15.1	−15.8	dE5	12:44:46	12:03:57	0.090	0.037
VCC2029	R964	18.2	−12.7	dE3	12:45:40	9:24:25	0.082	0.034

[1]FCC = Fornax Cluster Catalog, Ferguson 1989; VCC = Virgo Cluster Catalog, Binggeli, Sandage & Tammann 1985; LGC = Leo Group Catalog, Ferguson & Sandage 1990; apparent B magnitude and morphological types taken from these catalogs.

[2]NG = New Galaxy, IC = Index Catalog, UGC = Uppsala General Catalog of Galaxies, NGC= New General Catalog, R = Reaves 1983, DDO = David Dunlop Observatory Catalogue of Low Surface Brightness Galaxies

[3]Absolute B magnitudes calculated assuming $(M - m) = 30.0$ for Leo Group, 30.92 for Virgo Cluster, and 31.39 for the Fornax Cluster (Freedman et al. 2001). The values have not been corrected for foreground extinction.

[4]The Schlegel et al. 1998 values for foreground Galactic extinction, taken from the NASA/IPAC Extragalactic Database (NED), which is operated by the Jet Propulsion Laboratory, California Institute of Technology, under contract with the National Aeronautics and Space Administration.

Table 2.   Nucleated Dwarf Elliptical Galaxies

Galaxy	M_B	V^1	$V - I$	ϵ	r_0 ($''$)	r_0 (kpc)	M_V(nucleus)	$V - I$ (nucleus)	N_{GC} ^{2}
VCC1073	-16.7	13.89 ± 0.11	1.15 ± 0.03	0.30	8.6 ± 0.5	636.6	-11.24 ± 0.01	1.07 ± 0.02	16.7 ± 5.8
FCC136	-16.6	14.32 ± 0.18	1.12 ± 0.03	0.20	8.4 ± 1.3	641.9	-11.40 ± 0.01	1.05 ± 0.02	18.0 ± 5.3
VCC1386	-16.5	$\cdots$	1.06 ± 0.03	0.30	12.7 ± 0.1	945.3	-10.73 ± 0.04	0.88 ± 0.04	22.7 ± 6.1
VCC940	-16.1	$\cdots$	1.08 ± 0.03	0.16	10.8 ± 0.2	799.9	-11.16 ± 0.04	0.96 ± 0.04	52.4 ± 8.1
FCC324	-16.1	14.95 ± 0.10	1.10 ± 0.03	0.63	13.9 ± 0.3	1283.9	-8.80 ± 0.05	0.91 ± 0.05	9.0 ± 4.6
VCC1876	-16.0	14.39 ± 0.18	1.04 ± 0.03	0.49	10.5 ± 0.3	780.6	-10.40 ± 0.03	0.97 ± 0.02	22.1 ± 6.3
VCC1254	-15.9	14.82 ± 0.13	1.16 ± 0.03	0.03	7.7 ± 0.2	568.4	-12.25 ± 0.02	1.01 ± 0.02	20.5 ± 8.0
VCC949	-15.8	$\cdots$	1.11 ± 0.03	0.30	10.7 ± 0.3	793.2	-9.80 ± 0.04	0.93 ± 0.04	21.6 ± 5.5
VCC1308	-15.8	$\cdots$	1.05 ± 0.03	0.30	6.0 ± 0.4	443.7	-11.41 ± 0.04	1.05 ± 0.04	19.7 ± 5.9
VCC1514	-15.8	$\cdots$	1.00 ± 0.03	0.67	12.6 ± 0.3	932.0	-8.89 ± 0.04	0.92 ± 0.05	7.0 ± 4.4
VCC1107	-15.8	$\cdots$	1.12 ± 0.05	0.33	11.8 ± 0.3	871.8	-10.32 ± 0.04	0.96 ± 0.03	1.8 ± 2.5
FCC46	-15.8	$\cdots$	0.88 ± 0.03	0.38	5.3 ± 0.7	489.0	-12.16 ± 0.03	0.58 ± 0.04	8.0 ± 4.2
FCC150	-15.7	15.13 ± 0.10	1.05 ± 0.03	0.15	5.5 ± 0.3	502.9	-11.01 ± 0.02	1.03 ± 0.02	8.0 ± 4.2
VCC871	-15.5	$\cdots$	1.05 ± 0.03	0.33	10.8 ± 0.2	785.8	-9.10 ± 0.03	0.88 ± 0.05	15.6 ± 4.9
VCC965	-15.5	$\cdots$	1.02 ± 0.03	0.49	13.4 ± 0.3	990.6	-10.97 ± 0.04	0.92 ± 0.03	13.2 ± 4.6
VCC1311	-15.3	$\cdots$	1.03 ± 0.03	0.08	9.6 ± 0.3	713.8	-10.55 ± 0.03	0.90 ± 0.04	15.7 ± 4.7
VCC1497	-15.2	$\cdots$	1.04 ± 0.03	0.47	12.7 ± 0.5	945.3	-9.13 ± 0.05	0.89 ± 0.05	5.0 ± 4.6
VCC158	-15.1	$\cdots$	1.14 ± 0.03	0.33	12.5 ± 0.3	929.0	-10.08 ± 0.05	0.95 ± 0.05	3.0 ± 4.1
VCC452	-15.1	15.36 ± 0.11	1.06 ± 0.03	0.22	7.8 ± 0.4	579.5	-8.50 ± 0.04	0.91 ± 0.06	15.5 ± 5.3
VCC992	-15.1	$\cdots$	1.04 ± 0.06	0.08	7.8 ± 0.3	580.2	-9.20 ± 0.04	0.89 ± 0.04	12.5 ± 5.0
VCC1577	-15.1	15.17 ± 0.31	1.04 ± 0.03	0.24	7.1 ± 0.4	523.9	-8.64 ± 0.05	0.90 ± 0.04	8.9 ± 4.6
FCC174	-14.7	16.16 ± 0.1	0.97 ± 0.08	0.17	4.9 ± 0.5	454.1	-9.76 ± 0.02	0.92 ± 0.03	4.1 ± 3.4
FCC316	-14.7	16.17 ± 0.1	1.06 ± 0.03	0.30	8.2 ± 0.3	750.6	-9.49 ± 0.02	1.07 ± 0.03	8.0 ± 3.7
VCC1105	-14.7	$\cdots$	0.93 ± 0.17	0.14	10.3 ± 0.5	761.3	-9.82 ± 0.04	0.87 ± 0.04	14.0 ± 4.9
VCC747	-14.7	$\cdots$	$\cdots$	0.20	10.1 ± 0.7	747.2	-10.02 ± 0.03	0.88 ± 0.04	17.0 ± 5.6
VCC503	-14.1	16.83 ± 0.10	1.02 ± 0.15	0.06	6.3 ± 0.4	468.2	-9.06 ± 0.03	0.91 ± 0.03	2.5 ± 3.7
FCC254	-13.8	16.71 ± 0.21	1.07 ± 0.10	0.16	10.5 ± 0.5	967.1	-10.58 ± 0.01	0.91 ± 0.02	4.5 ± 4.2
FCC25	-13.7	$\cdots$	$\cdots$	0.25	6.1 ± 0.3	564.6	-9.88 ± 0.03	0.90 ± 0.04	2.5 ± 3.7
FCC242	-13.6	$\cdots$	$\cdots$	0.43	9.3 ± 0.6	852.8	-8.22 ± 0.05	0.94 ± 0.07	0.0 ± 2.7
LGC50	-13.3	16.04 ± 0.21	1.03 ± 0.03	0.36	10.2 ± 0.4	494.2	-8.50 ± 0.02	0.80 ± 0.03	7.2 ± 3.8
VCC896	-13.1	$\cdots$	0.98 ± 0.15	0.38	8.8 ± 0.6	655.9	-8.35 ± 0.04	0.99 ± 0.06	4.5 ± 3.9
VCC529	-12.7	$\cdots$	$\cdots$	0.43	6.6 ± 0.5	489.7	-9.67 ± 0.03	0.88 ± 0.04	2.0 ± 2.0
FCC238	-12.7	$\cdots$	$\cdots$	0.34	7.0 ± 0.7	644.7	-9.32 ± 0.03	0.89 ± 0.05	7.2 ± 4.1
VCC240	-12.7	16.34 ± 0.70	0.98 ± 0.10	0.35	9.5 ± 1.0	705.6	-9.46 ± 0.02	0.91 ± 0.03	3.5 ± 3.5
FCC189	-12.6	$\cdots$	$\cdots$	0.26	2.4 ± 0.3	222.0	-9.17 ± 0.03	0.81 ± 0.05	6.5 ± 4.2
VCC1530	-12.6	$\cdots$	$\cdots$	0.15	5.9 ± 0.3	440.7	-9.73 ± 0.03	0.84 ± 0.04	0.5 ± 3.4
VCC1714	-12.4	$\cdots$	$\cdots$	0.39	12.0 ± 0.8	893.4	-11.82 ± 0.02	0.55 ± 0.03	2.5 ± 3.4
VCC1272	-12.4	$\cdots$	$\cdots$	0.40	4.2 ± 0.4	308.7	-7.66 ± 0.05	0.69 ± 0.09	0.0 ± 3.8
FCC246	-12.3	$\cdots$	$\cdots$	0.38	6.6 ± 0.7	609.7	-7.28 ± 0.09	0.84 ± 0.13	0.0 ± 2.7
VCC646	-12.1	$\cdots$	$\cdots$	0.23	5.6 ± 0.2	414.1	-9.55 ± 0.03	0.96 ± 0.04	6.5 ± 4.2
VCC1252	-12.1	$\cdots$	$\cdots$	0.05	4.7 ± 0.5	345.0	-9.02 ± 0.03	0.86 ± 0.04	4.5 ± 3.9
FCC59	-12.0	$\cdots$	$\cdots$	0.38	11.0 ± 2.2	1016.8	-8.72 ± 0.04	0.83 ± 0.06	0.0 ± 3.2
VCC1363	-11.9	$\cdots$	$\cdots$	0.35	3.7 ± 0.2	271.6	-8.83 ± 0.03	0.89 ± 0.05	0.5 ± 2.7
FCC146	-11.9	$\cdots$	$\cdots$	0.49	3.3 ± 0.4	304.9	-8.11 ± 0.05	1.01 ± 0.08	0.0 ± 2.6
VCC1077	-11.7	$\cdots$	$\cdots$	0.18	3.7 ± 0.3	242.6	-8.45 ± 0.04	0.93 ± 0.05	1.5 ± 4.5

[1]From Stiavelli et al. 2001

[2]Corrected for background contamination

Table 3.   Non-nucleated Dwarf Elliptical Galaxies

Galaxy	M_B	V^1	$V - I$	ϵ	r_0 ($''$)	r_0(kpc)	$N_{GC}{}^2$
VCC9	−17.0	13.21 ± 0.10	1.00 ± 0.03	0.16	18.3 ± 0.6	1358.6	23.9 ± 6.9
VCC543	−16.1	⋯	1.07 ± 0.03	0.46	8.5 ± 0.7	630.0	13.0 ± 4.4
VCC917	−16.0	14.76 ± 0.10	1.01 ± 0.03	0.46	6.0 ± 0.2	443.0	6.0 ± 5.1
VCC1948	−15.8	⋯	0.99 ± 0.03	0.28	7.3 ± 0.1	540.9	6.5 ± 3.7
VCC2008	−15.8	⋯	1.00 ± 0.03	0.71	36.8 ± 0.9	2729.1	7.5 ± 5.1
VCC118	−15.3	15.55 ± 0.15	0.94 ± 0.03	0.22	8.0 ± 0.6	592.2	3.0 ± 3.6
VCC128	−15.3	⋯	1.10 ± 0.05	0.09	12.1 ± 0.6	898.6	11.1 ± 4.4
VCC546	−15.2	⋯	0.91 ± 0.03	0.61	10.6 ± 0.4	785.8	4.8 ± 3.3
LGC47	−15.1	14.57 ± 0.10	1.02 ± 0.03	0.13	12.9 ± 0.6	623.2	2.9 ± 4.4
VCC1762	−14.7	15.81 ± 0.20	0.97 ± 0.03	0.53	6.9 ± 0.2	504.6	4.0 ± 3.5
FCC110	−14.6	16.49 ± 0.10	1.14 ± 0.03	0.40	10.8 ± 0.4	994.7	0.0 ± 4.2
FCC48	−14.3	16.55 ± 0.13	1.00 ± 0.03	0.45	6.9 ± 0.4	631.8	7.0 ± 4.4
FCC64	−13.9	17.09 ± 0.10	1.12 ± 0.03	0.25	8.3 ± 0.7	767.2	0.0 ± 2.9
VCC1651	−13.9	16.08 ± 0.29	1.11 ± 0.11	0.44	19.2 ± 1.1	1424.6	4.2 ± 5.3
FCC212	−13.8	⋯	⋯	0.36	15.1 ± 0.8	1388.9	5.5 ± 5.3
VCC1729	−13.1	⋯	0.98 ± 0.03	0.47	6.3 ± 0.4	466.0	1.0 ± 3.0
FCC218	−12.9	⋯	⋯	0.31	5.6 ± 0.5	513.9	0.0 ± 2.7
VCC2029	−12.7	16.98 ± 0.28	1.00 ± 0.03	0.32	5.0 ± 0.3	463.3	1.0 ± 3.6
FCC304	−12.6	⋯	⋯	0.15	7.2 ± 0.9	660.4	0.0 ± 3.1
VCC996	−12.5	⋯	⋯	0.33	7.0 ± 0.4	517.9	0.0 ± 3.7
VCC1877	−12.3	⋯	⋯	0.43	7.4 ± 0.2	546.9	3.0 ± 3.3
VCC1781	−12.2	⋯	⋯	0.32	5.6 ± 0.4	417.7	2.5 ± 3.4
FCC144	−12.2	⋯	⋯	0.19	3.7 ± 0.4	337.1	0.5 ± 3.4
FCC27	−12.1	⋯	⋯	0.26	3.6 ± 0.5	334.3	0.5 ± 3.1

[1]From Stiavelli et al. 2001

[2]Corrected for background contamination.

Table 4.   Composite dE Globular Cluster Color Distributions

Magnitude Bin	N_{galaxy}	$\langle M_B \rangle$	N_{GC}	$\langle V-I \rangle$[1]	$\sigma(V-I)$[1]
$-11.7 > M_B > -13.0$	22	-12.4	28 ± 16	0.83 ± 0.02	0.03 ± 0.01
$-13.0 > M_B > -14.0$	9	-13.7	29 ± 12	0.84 ± 0.05	0.04 ± 0.03
$-14.0 > M_B > -15.0$	8	-14.7	54 ± 10	0.91 ± 0.03	0.07 ± 0.05
$-15.0 > M_B > -16.0$	21	-15.5	216 ± 22	0.89 ± 0.01	0.10 ± 0.02
$-16.0 > M_B > -17.0$	9	-16.1	194 ± 18	0.90 ± 0.01	0.13 ± 0.01

[1]Median Gaussian fit and standard deviation of fitted parameter for 10,000 bootstrap realizations of background-corrected GC color distributions.

Table 5.   Literature dE/dSph Globular Cluster System and Field Star Properties

Galaxy	M_B	M_V	N_{GC}	$\langle[\text{Fe/H}]\rangle_{GC}$	$\langle V-I \rangle_{GC}$	$\langle[\text{Fe/H}]\rangle_{FS}$	$\langle\text{Age}\rangle_{FS}$	Notes
					Local Group dSph/dE			
Fornax	-12.6	-13.1	5	-1.8 ± 0.2	0.83 ± 0.06	-0.9 ± 0.1	≤ 4 Gyr	1,2,3
Sagittarius	-12.8	-13.3	4	-1.6 ± 0.5	0.89 ± 0.14	-0.5 ± 0.1	6 ± 2 Gyr	1,4,5; includes Terzan7
NGC147	-14.8	-15.2	2	-2.0 ± 0.4	0.75 ± 0.12	$-0.9 \pm$?	≥ 4 Gyr	1,6,7
NGC185	-14.7	-15.5	5	-1.7 ± 0.3	0.86 ± 0.10	-1.2 ± 0.2	≥ 4 Gyr	1,6,8,9
NGC205	-16.0	-16.6	7	-1.4 ± 0.1	0.95 ± 0.04	-0.8 ± 0.2	~ 4 Gyr	1,6,10
VCC1254	-15.9	-16.1	22 ± 8	-1.5 ± 0.1	0.93 ± 0.06	-1.1 ± 0.2	$\cdots$	14
VCC1386	-16.5	-16.8	17 ± 5	-1.5 ± 0.2	0.93 ± 0.02	-0.8 ± 0.2	$\cdots$	14
NGC3115DW1	-17.0	-17.7	7/37	-1.0 ± 0.2	0.98 ± 0.02	-0.7 ± 0.3	$\cdots$	11,12,13; $\langle V-I \rangle_{GC}$ from 13

Note. — (1) Mateo 1998; (2) Strader et al. 2003; (3) Pont et al. 2004; (4) Montegriffo et al. 1998 and references therein; (5) Monaco et al. 2002; (6) Da Costa & Mould 1988; (7) Han et al. 1997; (8) Martinez-Delgado & Aparicio 1998; (9) Geisler et al. 1999; (10) Mould, Kristian, & Da Costa 1984; (11) Durrell et al. 1996a; (12) Puzia et al. 2001; (13) Kundu & Whitmore 2001b; (14) Durrell et al. 1996b
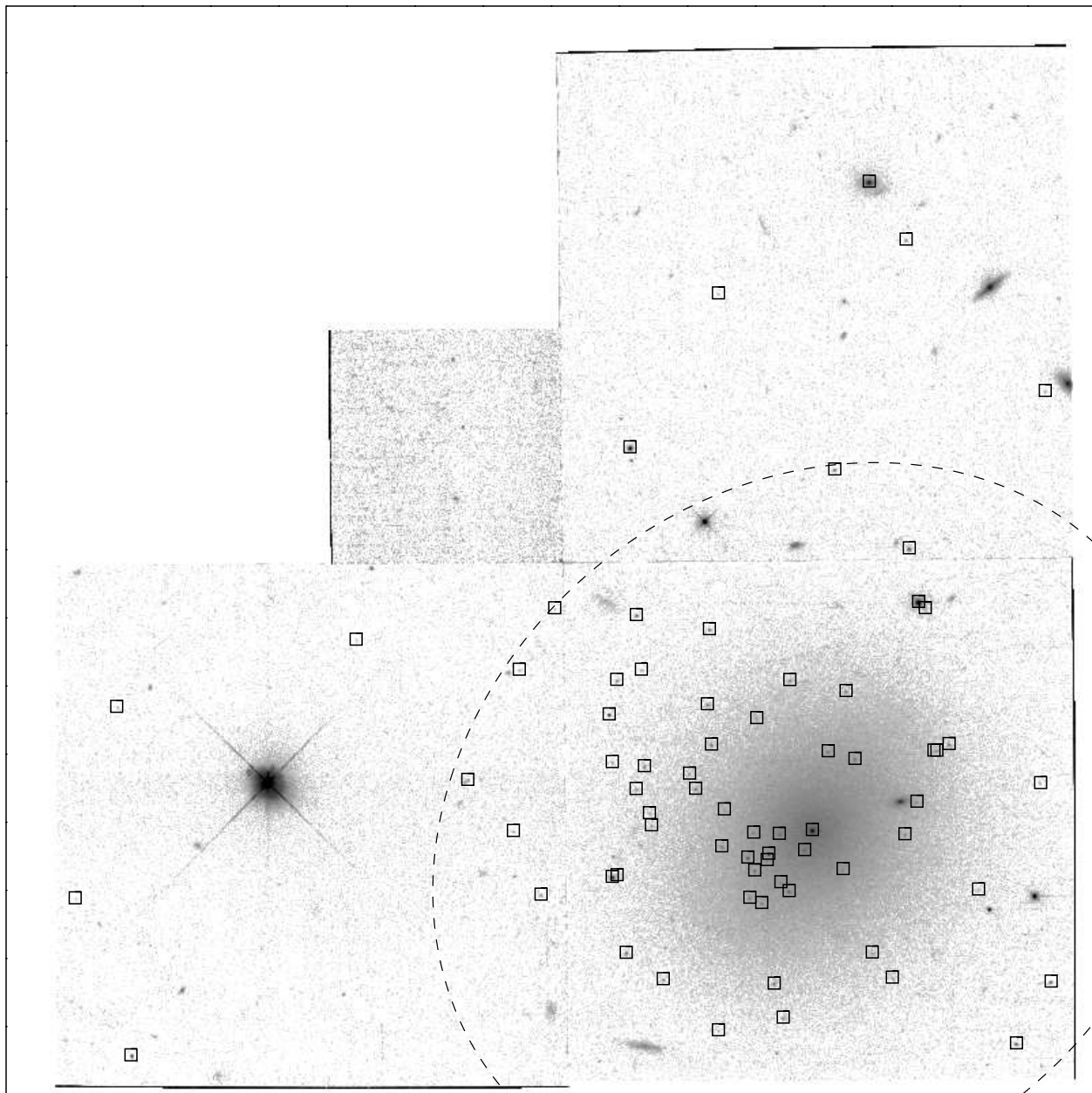
Fig. 1.— The WFPC2 F555W mosaic image of nucleated dE1 VCC940 ($M_B = -16.1$).
Compact sources meeting our globular cluster candidate criteria are boxed. Objects which
fall on WF3 or within 5 scalelengths of the center of the galaxy (dashed ellipse) are globular
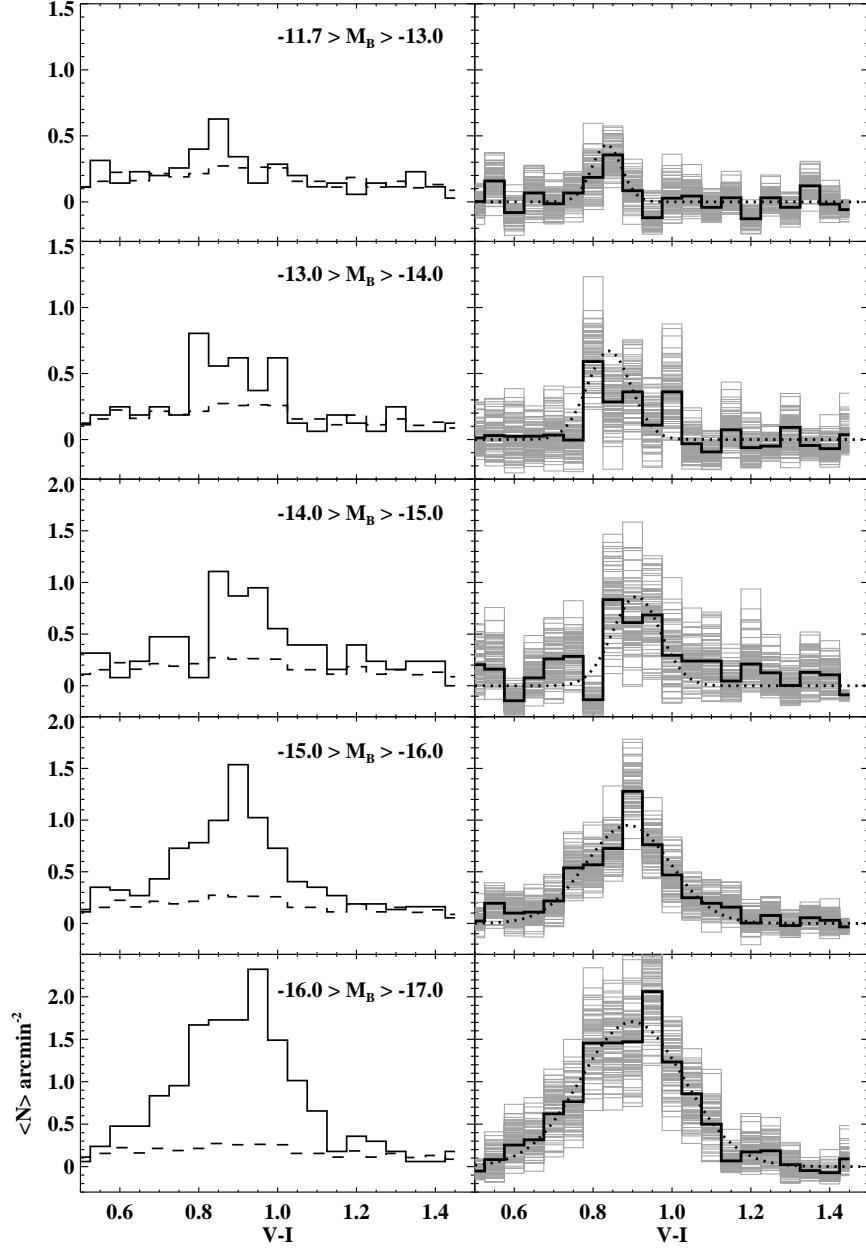cluster candidates. Objects outside of this radius are treated as background objects.

Fig. 2.— The composite globular cluster candidate color distribution as a function of host dE luminosity. Left: The raw galaxy GC (solid line) and background (dashed line) distributions. Right: The background corrected GC color distributions (heavy solid line), the first 100 bootstrapped GC color distributions (gray lines), and the median Gaussian fit to 10^4 bootstrapped color distributions (dotted curve).
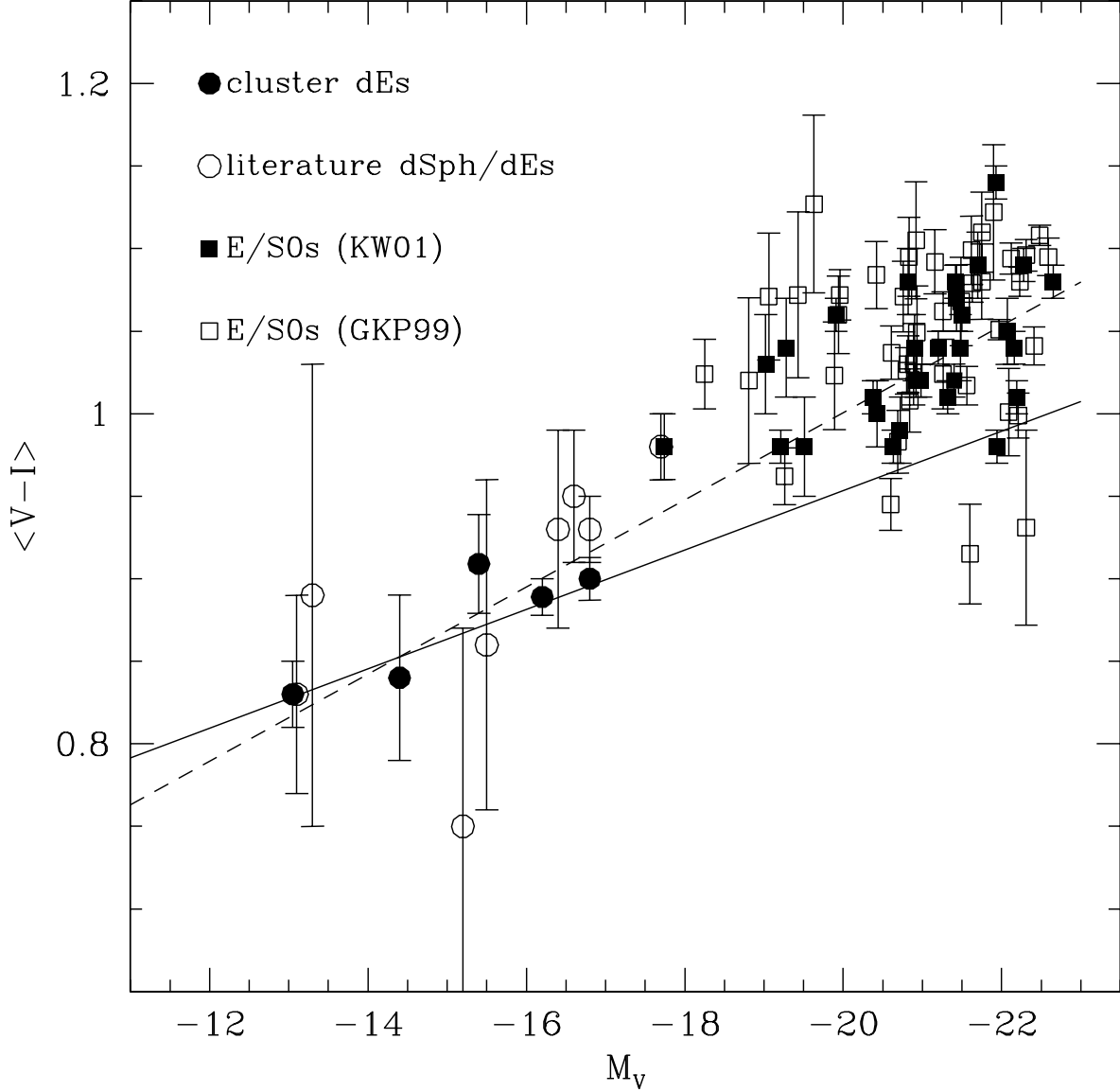
Fig. 3.— The peak globular cluster $V - I$ color v. host galaxy luminosity for our sample of Leo, Virgo and Fornax cluster dE GCS as well as nearby dE/dSphs, E and S0 GCS drawn from the literature (Table 5, KW01, GKP99). The error-bars here reflect the uncertainty in the peak of the color distribution. The lines are the linear fits to the dE $\langle V - I \rangle_{GC} - M_V$ correlation (solid: our dEs only; dashed: our dEs plus literature dEs/dSphs).
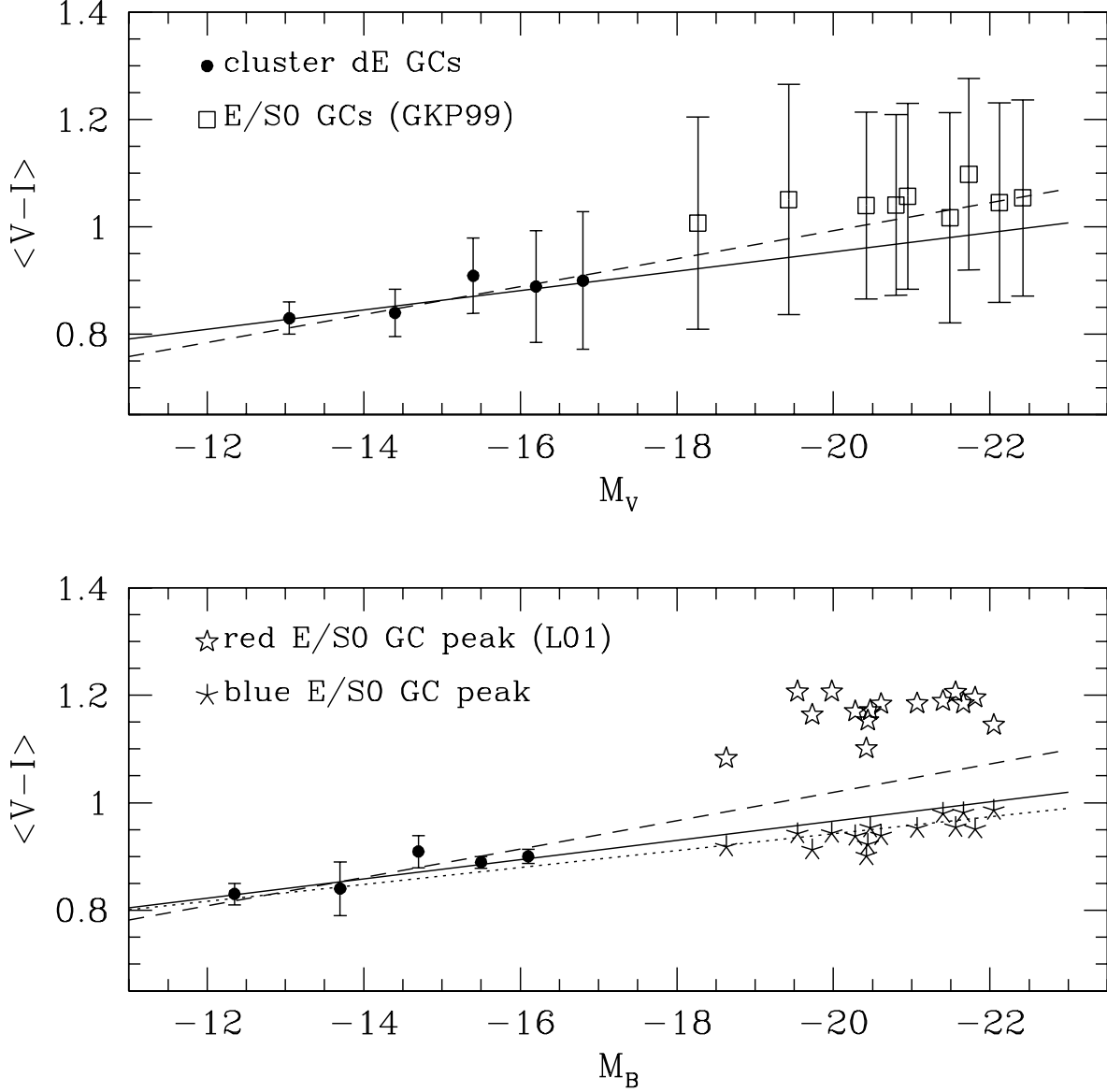
Fig. 4.— The dispersion in the globular cluster color distribution. *Top*: The peak $V - I$ values for the entire GCS v. host galaxy M_V. The error bars give the dispersion about this peak $\sigma(V - I)$. *Bottom:* The peak $V - I$ colors of the dE GCS and the red and blue peak colors of 16 E/S0s (Larson et al. 2001) v. host galaxy M_B. The solid and dashed lines are the linear fits to dE $\langle V - I \rangle_{GC} - M_V$ correlation, and the dotted line is the linear fit to blue E/S0 GCs from Larson et al.(2001). Here the error bars are standard errors of the mean.
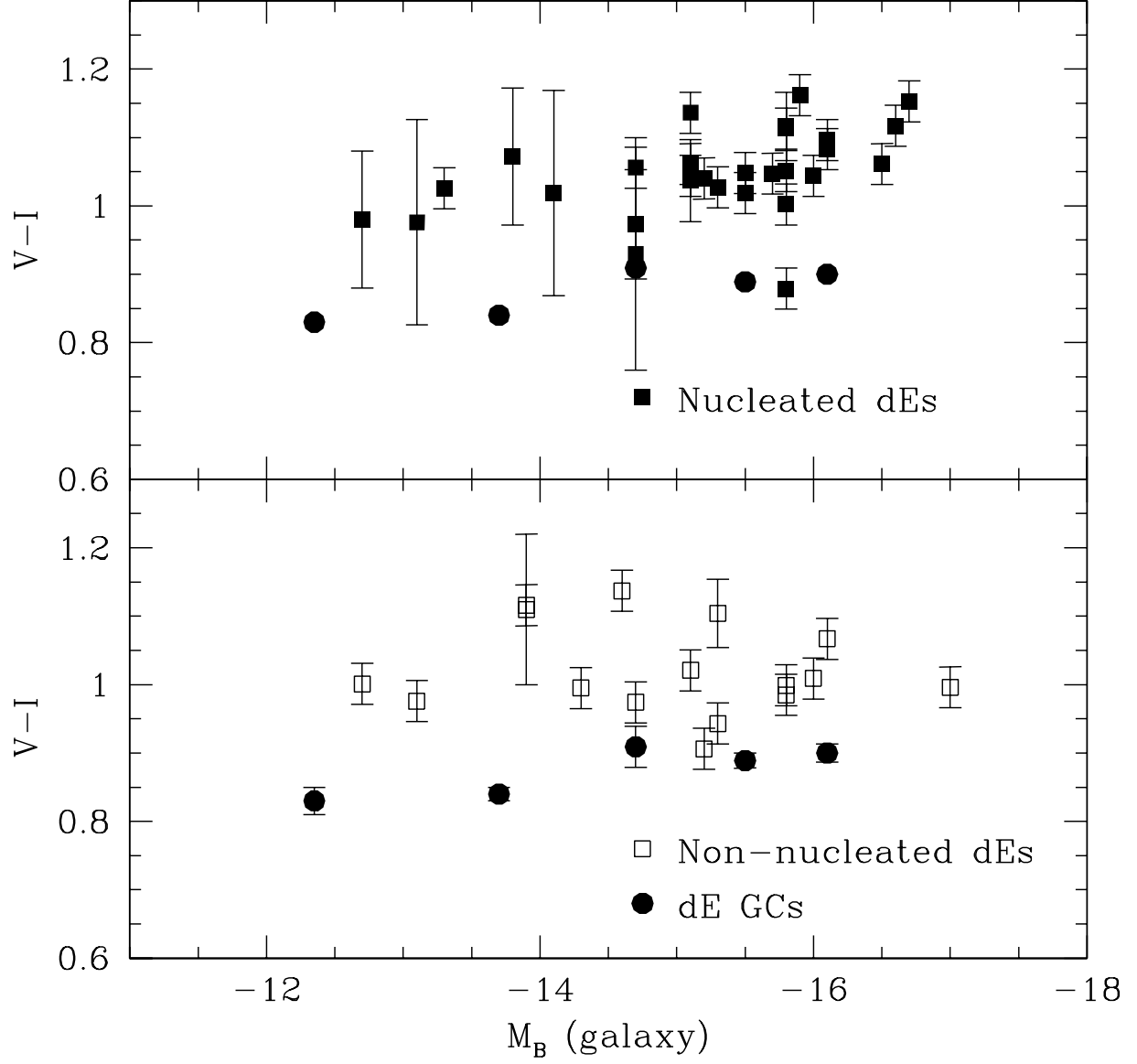
Fig. 5.— Nucleated (top) and non-nucleated (bottom) dE stellar halo colors v. host galaxy luminosity. The filled circles are the dE globular cluster colors from Figure 3.
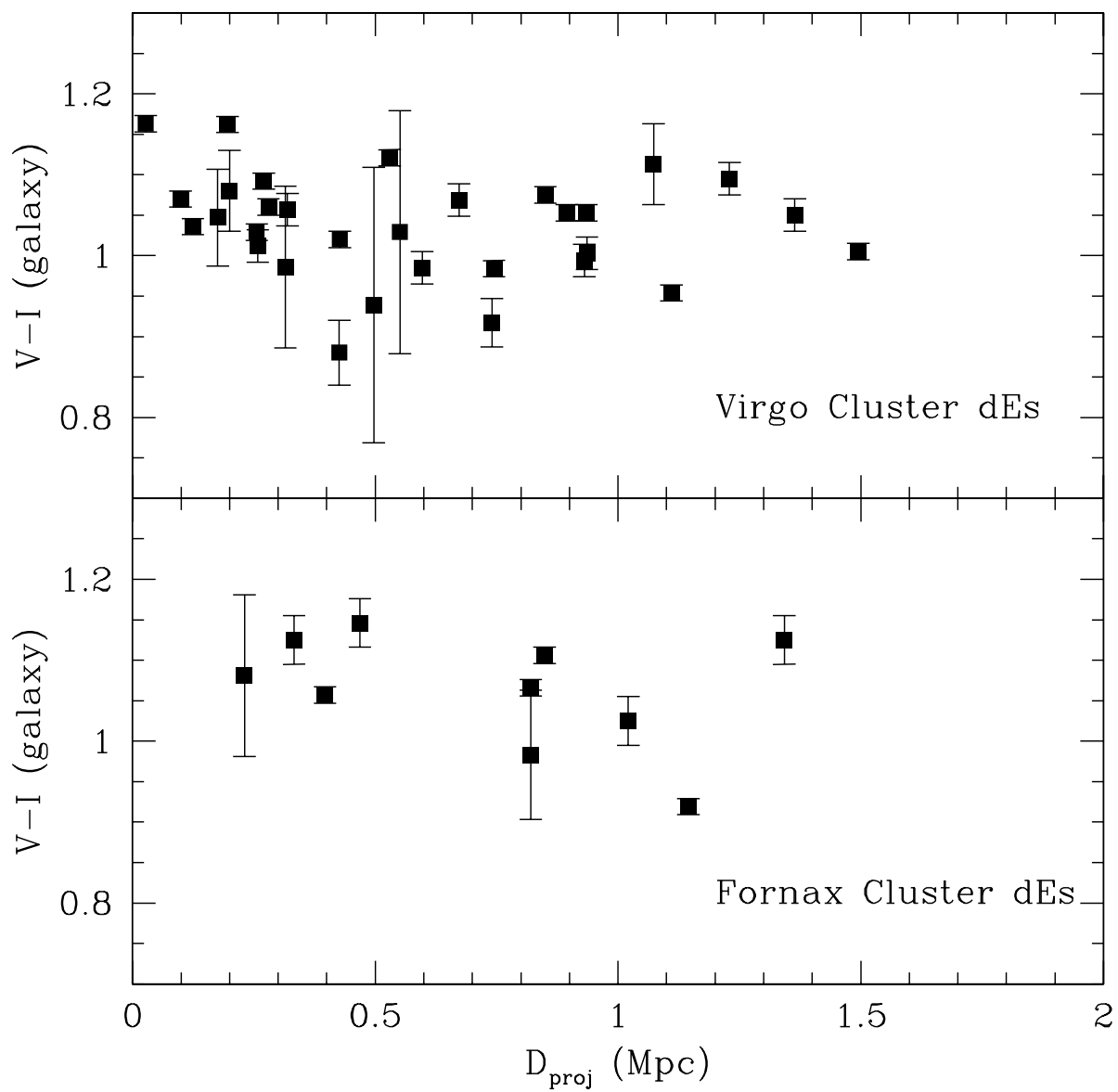
Fig. 6.— dE $V - I$ halo colors v. projected radius (Mpc) for Virgo and Fornax Cluster dEs.
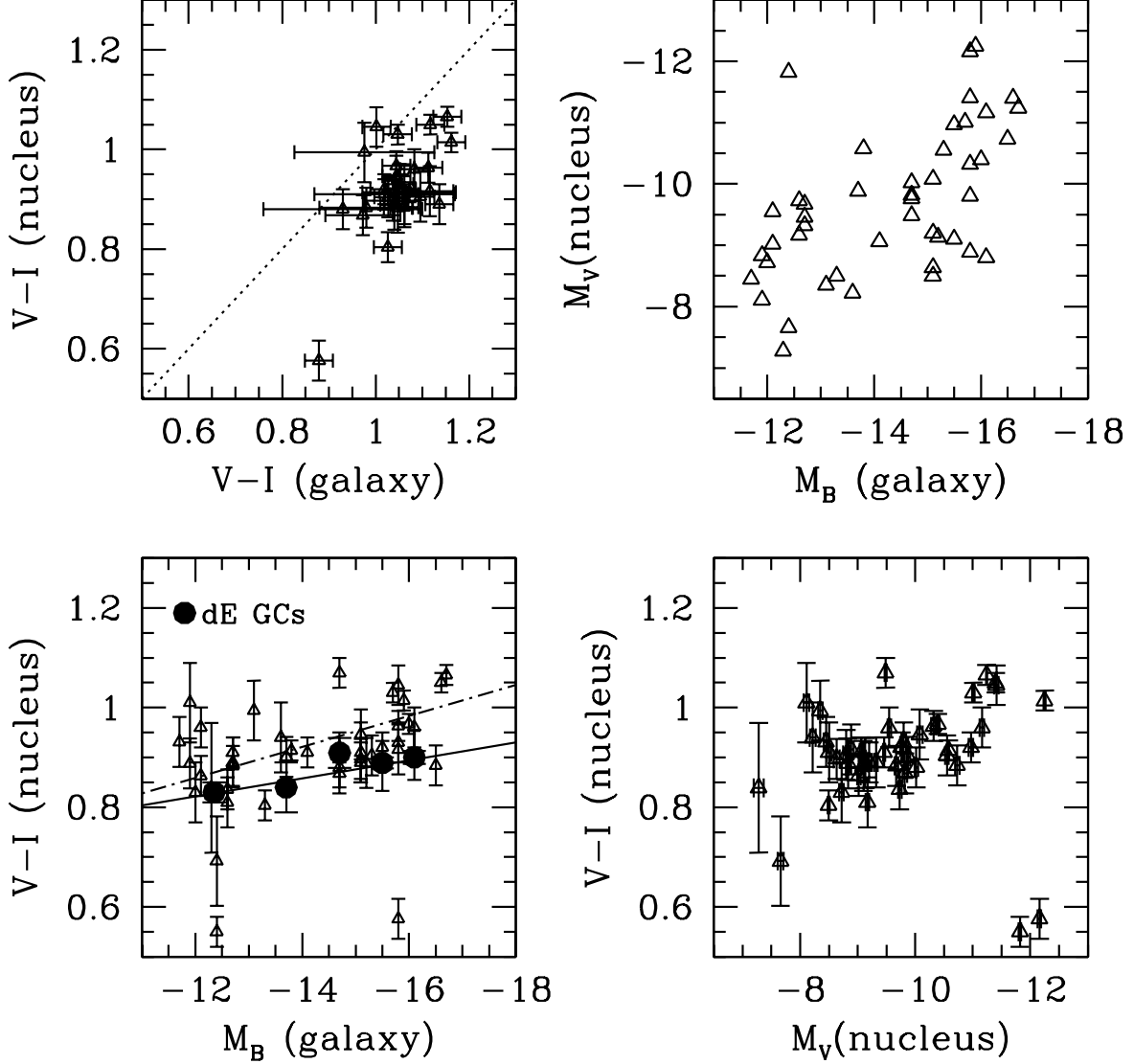
Fig. 7.— The dE nuclear properties. *Top left:* The nuclear $V - I$ color vs. host galaxy $V - I$ color. *Top right:* dE nuclear M_V vs. host galaxy M_B. The outlier at M_V (nucleus) $= -12$, M_B(galaxy) $= -12.5$ is the very blue nucleus of VCC1714. *Bottom left:* The dE nuclear colors (triangles) and peak globular cluster colors (circles) vs. host galaxy luminosity. The solid line is the fit to the dE GCs, and the dot-dashed line is the linear fit to the dE nuclei excluding the two blue outliers. *Bottom right:* Nuclear $V - I$ colors vs. nuclear M_V.
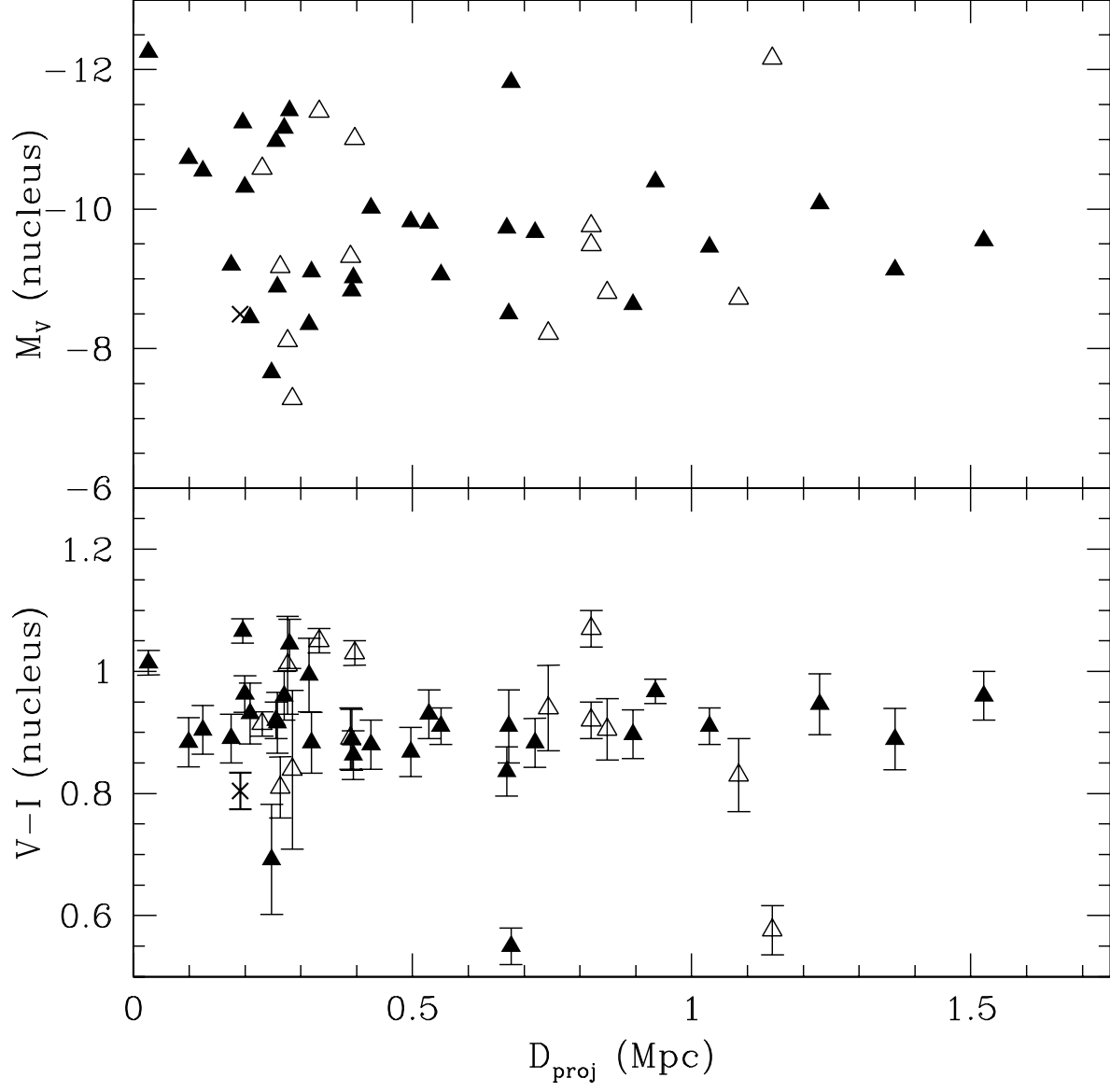
Fig. 8.— Nuclear properties v. host dE's projected distance from the cluster center. (filled triangles: Virgo Cluster, open triangles: Fornax Cluster, crosses: Leo Group)
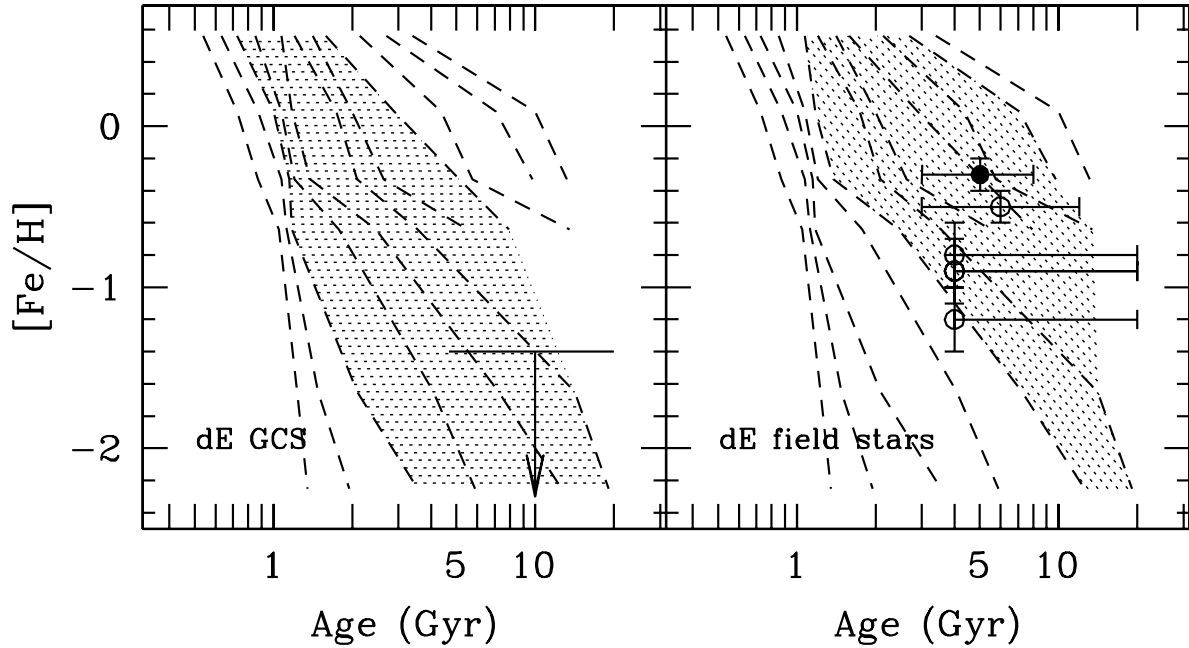
Fig. 9.— The age-metallicity constraints on the dE stellar populations from the $V - I$ colors and Bruzual & Charlot (2003) single burst population synthesis models. The dashed lines are lines of constant $V - I$ color ($V - I = 0.7 - 1.20$ in 0.05 intervals from left to right). *Left:* the range of dE GCS colors (shaded region) and the [Fe/H] and age constraints for Local Group dSph/dE old GCs (Table 5) are shown. *Right:* the shaded region shows the range of dE stellar halo colors ($0.9 \leq V - I \leq 1.15$). The mean spectroscopic result from Geha et al. (2003) for 17 Virgo and Fornax dEs is plotted as the solid circle. The constraints for the field stars in the Local Group dSphs/dEs from Table 5 are plotted as open circles.
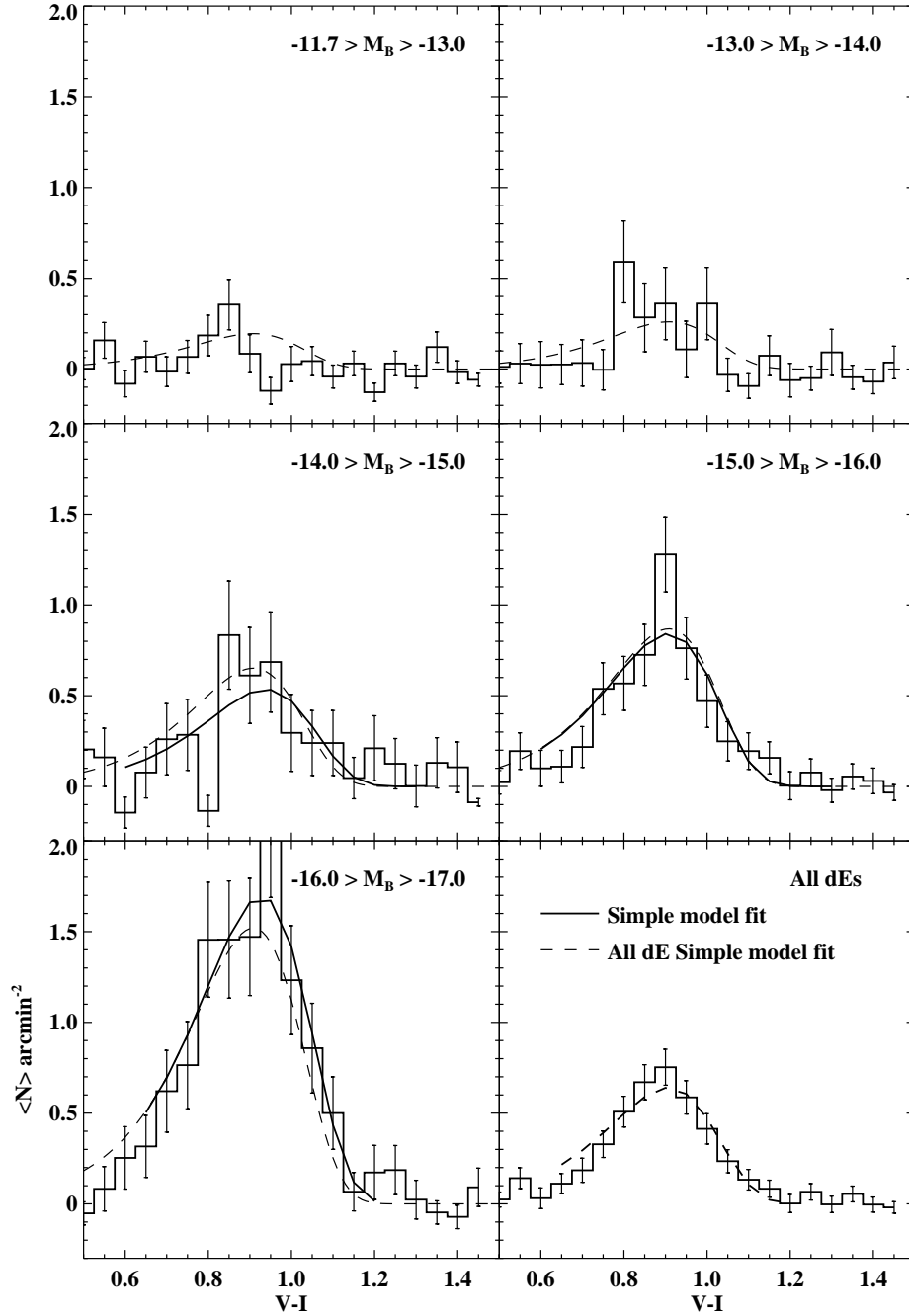
Fig. 10.— Simple model fits to the dE GC color distributions, assuming Kissler-Patig et al. (1998) $V - I$ to [Fe/H] calibration. The solid curves are the best fits for each histogram, and the dashed curves are from the best fit to all dE GCCs (lower right) for comparison. No reliable fits were found for the faintest GC color distributions (top panels).